PLOS ONE

RESEARCH ARTICLE

The Role of Neutrophil Proteins on the Amyloid Beta-RAGE Axis

Amanda J. Stock[1,2], Anne Kasus-Jacobi[1,2], Jonathan D. Wren[3,4], Virginie H. Sjoelund[5], Glenn D. Prestwich[6], H. Anne Pereira[1,2,7,8]*

1 Oklahoma Center for Neuroscience, University of Oklahoma Health Sciences Center, Oklahoma City, Oklahoma, United States of America, **2** Department of Pharmaceutical Sciences, University of Oklahoma Health Sciences Center, Oklahoma City, Oklahoma, United States of America, **3** Arthritis and Clinical Immunology Research Program, Oklahoma Medical Research Foundation, Oklahoma City, Oklahoma, United States of America, **4** Department of Biochemistry and Molecular Biology, University of Oklahoma Health Sciences Center, Oklahoma City, Oklahoma, United States of America, **5** Core Laboratory for Molecular Biology and Cytometry Research, University of Oklahoma Health Sciences Center, Oklahoma City, Oklahoma, United States of America, **6** Department of Medicinal Chemistry, University of Utah, Salt Lake City, Utah, United States of America, **7** Department of Pathology, University of Oklahoma Health Sciences Center, Oklahoma City, Oklahoma, United States of America, **8** Department of Cell Biology, University of Oklahoma Health Sciences Center, Oklahoma City, Oklahoma, United States of America

* Anne-Pereira@ouhsc.edu

Citation: Stock AJ, Kasus-Jacobi A, Wren JD, Sjoelund VH, Prestwich GD, Pereira HA (2016) The Role of Neutrophil Proteins on the Amyloid Beta-RAGE Axis. PLoS ONE 11(9): e0163330. doi:10.1371/journal.pone.0163330

Editor: Eliseo A Eugenin, Rutgers University, UNITED STATES

Received: May 5, 2016

Accepted: September 6, 2016

Published: September 27, 2016

Data Availability Statement: All relevant data are within the paper.

Funding: This study was supported through Public Health Service Grant 5R01EY015534 from the National Eye Institute (HAP) and the Oklahoma Center for the Advancement of Science and Technology (OCAST) HR12-068 (HAP). The funders had no role in study design, data collection and analysis, decision to publish, or preparation of the manuscript.

Competing Interests: Authors AJS, JDW and VHS have declared that no competing interests exist.

Abstract

We previously showed an elevated expression of the neutrophil protein, cationic antimicrobial protein of 37kDa (CAP37), in brains of patients with Alzheimer's disease (AD), suggesting that CAP37 could be involved in AD pathogenesis. The first step in determining how CAP37 might contribute to AD pathogenesis was to identify the receptor through which it induces cell responses. To identify a putative receptor, we performed GAMMA analysis to determine genes that positively correlated with CAP37 in terms of expression. Positive correlations with ligands for the receptor for advanced glycation end products (RAGE) were observed. Additionally, CAP37 expression positively correlated with two other neutrophil proteins, neutrophil elastase and cathepsin G. Enzyme-linked immunosorbent assays (ELISAs) demonstrated an interaction between CAP37, neutrophil elastase, and cathepsin G with RAGE. Amyloid beta 1–42 ($A\beta_{1-42}$), a known RAGE ligand, accumulates in AD brains and interacts with RAGE, contributing to $A\beta_{1-42}$ neurotoxicity. We questioned whether the binding of CAP37, neutrophil elastase and/or cathepsin G to RAGE could interfere with $A\beta_{1-42}$ binding to RAGE. Using ELISAs, we determined that CAP37 and neutrophil elastase inhibited binding of $A\beta_{1-42}$ to RAGE, and this effect was reversed by protease inhibitors in the case of neutrophil elastase. Since neutrophil elastase and cathepsin G have enzymatic activity, mass spectrometry was performed to determine the proteolytic activity of all three neutrophil proteins on $A\beta_{1-42}$. All three neutrophil proteins bound to $A\beta_{1-42}$ with different affinities and cleaved $A\beta_{1-42}$ with different kinetics and substrate specificities. We posit that these neutrophil proteins could modulate neurotoxicity in AD by cleaving $A\beta_{1-42}$ and influencing the Aβ1–42 –RAGE interaction. Further studies will be required to determine the biological significance of these effects and their relevance in neurodegenerative diseases

Author GDP has declared equity in GlycoMira. Author AKJ has received funding from the Oklahoma Center for Advancement of Science and Technology and National Institute of General Medical Sciences. Author HAP has declared equity in Biolytx Pharmaceuticals Corp and funding obtained through the National Eye Institute, National Institute of General Medical Sciences and the Oklahoma Center for the Advancement of Science and Technology for support of this study. This does not alter our adherence to PLOS ONE policies on sharing data and materials.

such as AD. Our findings identify a novel area of study that underscores the importance of neutrophils and neutrophil proteins in neuroinflammatory diseases such as AD.

Introduction

Neutrophil proteins are essential components of the innate immune system, and contribute to host defense by stimulating cytokine production, destroying invading pathogens, and recruiting other immune cells to sites of infection and inflammation [1–4]. Although the brain is considered an immune privileged site where minimal inflammatory responses can be elicited [5, 6] a number of immune mediators including neutrophil proteins have been detected in the brain parenchyma. Studies have shown increased levels of neutrophil proteins such as myeloperoxidase [7] and α-defensins 1 and 2 [8] in patients with neuroinflammatory diseases, including Alzheimer's disease (AD). Our lab previously observed the increased expression of the neutrophil cationic antimicrobial protein of 37kDa (CAP37) in cerebrovascular endothelial cells in the hippocampus of AD patients [9]. In a more recent study, we demonstrated the upregulation of CAP37 expression in cortical pyramidal neurons of AD patients [10]. We also observed cerebral expression of neutrophil elastase and cathepsin G, two other neutrophil proteins with sequence homology to CAP37. Increased expression of CAP37 was found in the brains of patients with AD compared with normal age matched controls, whereas levels of neutrophil elastase and cathepsin G were not elevated in AD patients [10]. These observations led to our hypothesis that CAP37 was a likely player in the neuroinflammatory process underlying AD.

One way that CAP37 and other neutrophil proteins could mediate neuroinflammation is by activating inflammatory receptors. Microglia are the predominant cells that regulate inflammatory responses in the brain. A previous report from our lab demonstrated that CAP37 was a potent modulator of microglial functions [2], indicating that a receptor for CAP37 may exist on microglial cells. Much is still unknown regarding the specific mechanisms of cell responses induced by CAP37-receptor-mediated interactions, and the identity of the CAP37 receptor(s) in the brain remains elusive. By performing a gene correlation analysis called GAMMA [11], we could determine genes that positively correlated with CAP37 and obtain clues for potential CAP37 receptors. Results obtained from GAMMA analysis prompted us to investigate interactions between CAP37 and the receptor for advanced glycation end products (RAGE).

RAGE is an inflammatory receptor expressed on various brain cells, including microglia, endothelial cells, astrocytes, and neurons [12]. RAGE expression is high in neurons during development, but expression is low in brain cells of adults during normal physiological conditions [12]. A number of ligands for RAGE have been identified, including advanced glycation end products (AGEs), which are well known for their role in diabetes and athlerosclerosis, inflammatory mediators such as members of the S100/calgranulin family, high mobility group box 1 protein (HMGB-1), the Mac-1 integrin, and amyloid beta (Aβ), found in the senile plaques of AD brains [13–15]. RAGE activation by its ligands initiates a positive feedback loop of inflammation by inducing de novo synthesis of NF-κBp65 mRNA and protein, and in this way contributes to chronic production of pro-inflammatory cytokines, up-regulation of RAGE, and inflammation [13, 16]. This chronic inflammatory response has been reported to occur in many neuroinflammatory diseases including AD. Furthermore, RAGE expression is increased in the brains of patients with AD [17], allowing for increased Aβ-RAGE signaling.

The general consensus is that Aβ is a major factor augmenting the neurotoxicity and cognitive decline observed in patients with AD [18]. The two most prevalent forms of Aβ are amyloid

beta 1–40 ($A\beta_{1-40}$) and amyloid beta 1–42 ($A\beta_{1-42}$). $A\beta_{1-42}$ is the most toxic species that accumulates in the brains of AD patients [19]. RAGE activation by $A\beta_{1-42}$ induces oxidative stress in cerebral endothelial cells and astrocytes by stimulating NADPH oxidase to produce reactive oxygen species (ROS) [20, 21]. The Aβ-RAGE interaction also induces NFκB activation on neurons and microglia which contributes to a pro-inflammatory environment [22, 23].

In the current study, we investigated binding of CAP37 to RAGE, and measured binding of neutrophil elastase and cathepsin G to RAGE for comparison. Additionally, we investigated the effects of CAP37, neutrophil elastase, and cathepsin G on the interaction of RAGE with amyloid beta (Aβ). Disruption of the $A\beta_{1-42}$ -RAGE interaction could be neuroprotective by decreasing oxidative stress and inflammation in the AD brain. On the other hand, enhancing this interaction could accelerate neurotoxicity. Understanding the effects of neutrophil proteins on the $A\beta_{1-42}$ -RAGE axis could be important for developing neuroprotective AD therapeutics.

Materials and Methods

Materials

Recombinant human RAGE Fc chimera was purchased from R&D Systems Inc. (Minneapolis, MN). CAP37, cathepsin G, and neutrophil elastase purified from human neutrophils were purchased from Athens Research & Technology (Athens, GA). All neutrophil proteins were determined by the manufacturer to be >95% pure by SDS-PAGE. For purified CAP37, chromogenic activity assays using synthetic substrates specific for either neutrophil elastase or cathepsin G were performed by the manufacturer to rule out the presence of neutrophil elastase and cathepsin G. Activity assays were also performed to confirm the absence of cathepsin G in purified neutrophil elastase and vice versa. Essentially fatty acid free bovine serum albumin (BSA, cat# A3803) was from Sigma Aldrich (St. Louis, MO). Amyloid beta ($A\beta_{1-42}$) purchased from American Peptide Company (Sunnyvale, CA) and Bachem (Torrance, CA) was determined to be 95.6% and 95.2% pure by HPLC analysis, respectively. The RAGE antagonist used was a new class of sulfated anionic polysaccharide semi-synthetic glycosaminoglycan ethers known as GM-0111 [24]. Protease inhibitor cocktail tablets were purchased from Roche Life Science (Indianapolis, IN) and used at 1X concentration. The primary antibodies used were monoclonal mouse anti-amyloid precursor protein/amyloid beta (APP/Aβ, #2450, Cell Signaling, Danvers, MA), polyclonal goat anti-RAGE (#AF1145, R&D Systems), and polyclonal rabbit anti-RAGE (#ab37647, Abcam, Cambridge, MA). Rabbit anti-goat secondary antibody conjugated to horseradish peroxidase (HRP) was purchased from Pierce (Rockford, IL). Donkey anti-mouse and donkey anti-rabbit secondary antibodies conjugated to HRP were purchased from Jackson ImmunoResearch Laboratories (West Grove, PA).

GAMMA

Global Microarray Meta-Analysis (GAMMA) [11] was used to identify genes that positively correlated with CAP37 (gene expressions are increased or decreased concomitantly) across heterogeneous datasets. GAMMA used the entire curated set (GDS files) of 3,900 2-color human microarray datasets downloaded from NCBI's GEO database [25] and normalized. The 20 most correlated genes were then analyzed for established shared protein-protein interactions (PPIs) within the Human Protein Reference Database (HPRD) [26].

ELISAs

$A\beta_{1-42}$ used for ELISAS was purchased from Bachem, dissolved in 1 mM sodium hydroxide, aliquoted, and kept at -20°C until used. Nunc Maxisorp 96 well plates (VWR, Radnor, PA) were

coated with 100 μL of phosphate buffered saline (PBS, pH 7.4) containing the stated concentrations of CAP37, neutrophil elastase, cathepsin G, $A\beta_{1-42}$, RAGE, or BSA for 3 h at room temperature and then overnight at 4°C. The plates were washed three times with PBS containing 0.05% tween (PBST), and then blocked in PBST containing 3% bovine serum albumin (BSA). Indicated proteins were added to the plate in 50 μL PBST containing 0.1% BSA and incubated at 37°C for 70 mins. Wells were washed four times with PBST, and then incubated with 50 μL of goat anti-RAGE primary antibody (0.5 μg/ml) or mouse anti-APP/Aβ antibody (0.5 μg/ml-1 μg/ml) for 1 h. After washing the wells four times with PBST, 50 μL of rabbit anti-goat at 0.16 μg/ml or donkey anti-mouse at 0.04–0.08 μg/ml secondary antibodies were added for 1 h at room temperature. Wells were washed with PBST before using o-phenylenediamine (OPD) substrate (Sigma-Aldrich) to develop a colorimetric reaction based on the amount of bound RAGE or $A\beta_{1-42}$. Plates were incubated with OPD substrate for 10–30 minutes in the dark before adding 2.5M H_2SO_4 to stop the reaction, and a Synergy 2 multi-detection microplate reader (Biotek Instrument Inc.,Winooski, VT) was used to measure absorbance at 492 nm.

Binding of RAGE to neutrophil proteins. In one set of experiments aimed to determine the binding of RAGE to CAP37, neutrophil elastase, and cathepsin G, maxisorp plates were coated with CAP37 (0.5 μg/well, 208 nM), neutrophil elastase (0.5 μg/well, 192 nM), cathepsin G (0.5 μg/well, 200 nM), $A\beta_{1-42}$ (0.5 μg/well, 1 μM), or BSA (1000 μg/well, 152 μM) overnight at 4°C. Recombinant human RAGE Fc chimera (0–0.01 μg/well, 0–3.3 nM) that pre-incubated in the presence or absence of an excess of RAGE antagonist, GM-0111 (0.25 μg/ml, 50 nM) with rotation overnight at 4°C, was added to wells of the coated plate. Goat anti-RAGE primary antibody at 0.5 μg/ml was used to detect bound RAGE.

Competitive inhibition of $A\beta_{1-42}$ binding to RAGE by neutrophil proteins. In another set of experiments aimed to determine if the neutrophil proteins could competitively inhibit the binding of $A\beta_{1-42}$ to RAGE, the maxisorp plates were coated with RAGE Fc chimera (0.5 μg/well, 83.3 nM) overnight at 4°C. The next day $A\beta_{1-42}$ (0.0025 μg/well, 11 nM) ± a protease inhibitor cocktail was added to respective wells at the same time as varying concentrations of CAP37 (0–3 μg/well, 0–2.5 μM) or neutrophil elastase (0–0.65 μg/well, 0–0.5 μM).

Determine if neutrophil proteins interact with $A\beta_{1-42}$ to prevent it from binding to RAGE. Another set of ELISA experiments were performed to determine if the amyloid beta-RAGE interaction could be inhibited by pre-incubation of $A\beta_{1-42}$ with neutrophil proteins. In this set of experiments, the maxisorp plates were coated with RAGE Fc chimera (0.5 μg/well, 83.3 nM) overnight at 4°C. $A\beta_{1-42}$ (0–0.05 μg/well, 0–222 nM) was pre-incubated with rotation overnight at 4°C in the presence or absence of CAP37 (0.025–0.1 μg/well, 21–83 nM) or neutrophil elastase (0.025–0.1 μg/well, 20–80 nM) and added to the coated plate. Mouse anti-APP/Aβ (1 μg/ml) was used to detect bound $A\beta_{1-42}$.

Binding of $A\beta_{1-42}$ to neutrophil proteins. In a final set of ELISA experiments aimed to determine the binding of $A\beta_{1-42}$ to CAP37, neutrophil elastase, and cathepsin G, maxisorp plates were coated with CAP37 (0.5 μg/well, 208 nM), neutrophil elastase (0.5 μg/well, 192 nM), cathepsin G (0.5 μg/well, 200 nM), or BSA (1000 μg/well, 152 μM). The next day varying concentrations of $A\beta_{1-42}$ (0–0.025 μg/well, 0–111 nM) in PBST buffer containing 0.1% BSA and a protease inhibitor cocktail was added to determine the binding of $A\beta_{1-42}$ to CAP37, neutrophil elastase, or cathepsin G. Mouse anti-APP/Aβ at 0.5 μg/ml was used to detect bound $A\beta_{1-42}$.

Far-Western dot Blotting

$A\beta_{1-42}$ used for far-Western dot blotting was purchased from Bachem, dissolved in 1 mM sodium hydroxide, aliquoted, and stored at -20°C until used. The stated concentrations of CAP37, neutrophil elastase, cathespin G, $A\beta_{1-42}$, or BSA were each combined with 150 μL PBS

and spotted through wells of a BIO-DOT apparatus (Bio-Rad, Hercules, CA) onto nitrocellulose membranes pre-soaked in PBS. After spotting, membranes were rinsed with ultrapure water, and Ponceau S (Sigma Aldrich) was used to stain for spotted proteins. Ponceau S was rinsed off with ultrapure water, and membrane blots were blocked for 2 h at room temperature in PBST containing 3% BSA. Blots were incubated with the indicated proteins (RAGE or $A\beta_{1-42}$) diluted in PBST containing 0.1% BSA overnight with rocking at 4°C. Blots were washed three times with PBST for 10 min, and then incubated with either rabbit anti-RAGE primary antibody (0.8μg/ml) or mouse anti-APP/Aβ (0.25μg/ml) for 2 h at room temperature. Blots were washed three times with PBST for 10 min, and then incubated with donkey anti-rabbit or donkey anti-mouse secondary antibodies at 0.04μg/ml for 45 min at room temperature. Blots were washed three times with PBST. Enhanced chemiluminescent or SuperSignal West femto maximum sensitivity substrates (Pierce) were used to develop blots. Mean dot densities were quantified and normalized to ponceau S dot densities using Image J software (National Institutes of Health (NIH), Bethesda, MD).

Binding of RAGE to neutrophil proteins. To determine binding of RAGE to neutrophil proteins using far-Western dot blot analysis, 0.5 μg $A\beta_{1-42}$ (as a positive control) and 1 μg of CAP37, neutrophil elastase, cathepsin G, and BSA were each spotted in quadruplicate using a BIO-DOT apparatus onto nitrocellulose membranes pre-soaked in PBS. Membranes were cut to make two blots (one for RAGE and one for RAGE+GM-0111) that each contained duplicate spots for each protein. After blocking, blots were incubated overnight at 4°C with recombinant human RAGE Fc chimera (0.25μg/ml, 4.2nM) that pre-incubated in the presence or absence of RAGE antagonist GM-0111 (0.625μg/ml, 125nM) with rotation overnight at 4°C. Rabbit anti-RAGE primary antibody at 0.8 μg/ml was used to detect bound RAGE.

Binding of $A\beta_{1-42}$ to neutrophil proteins. To determine binding of $A\beta_{1-42}$ to neutrophil proteins using far-Western dot blot analysis, 1 μg of CAP37, neutrophil elastase, cathepsin G, and BSA were each spotted in triplicate using a BIO-DOT apparatus onto nitrocellulose membranes pre-soaked in PBS. After blocking, $A\beta_{1-42}$ was added at 0.25μg/ml (56nM) in PBST containing 0.1% BSA and a protease inhibitor cocktail. Blots were incubated with rocking overnight at 4°C. Mouse anti-APP/Aβ at 0.25μg/ml was used to detect bound $A\beta_{1-42}$.

Mass Spectrometry

$A\beta_{1-42}$ used for mass spectrometry was purchased from American Peptide Company, dissolved in 0.05M Tris buffer, pH 8.0, aliquoted, and kept at -20°C until used. Samples ($A\beta_{1-42}$ alone, or $A\beta_{1-42}$ incubated with CAP37, neutrophil elastase, or cathepsin G) were analyzed by matrix-assisted laser-desorption/ionization mass spectrometry (MALDI-TOF MS). Concentrations of $A\beta_{1-42}$, CAP37, neutrophil elastase, and cathepsin G used were ~75 μM, 28 μM, 7 μM, and 7 μM, respectively. All samples were incubated ± protease inhibitor cocktail. The protease inhibitor cocktail and each protein by itself were analyzed to distinguish between peaks derived from the protease inhibitors or neutrophil proteins and the peaks generated from Aβ cleavage. All samples incubated in a 1:1 volume ratio of Tris buffer pH 8.0 (containing $A\beta_{1-42}$ or not) and sodium buffer, pH 5.5 (containing neutrophil protein or not). The sodium buffer contained 50 mM Na acetate and 150 mM NaCl. Samples were analyzed immediately after combining the neutrophil proteins with $A\beta_{1-42}$ at room temperature ($t \approx 0.25$ min), after incubation at room temperature with CAP37 for 1–300 min, or after incubation at room temperature with neutrophil elastase or cathepsin G for 1–60 min. Saturated sinapinic acid was dissolved in TA30 solvent (70:30 volume ratio of 0.1% trifluoroacetic acid: acetonitrile) at 10mg/ml and was deposited onto a MTP 384-spot ground steel target plate TF, to serve as matrix and allowed to dry. Following this, the samples were combined at a 1:1 ratio with sinapinic acid solution,

deposited onto respective matrix spots on the target plate, and allowed to dry. The samples were analyzed with a Bruker Ultraflex II TOF/TOF mass spectrometer (Ultraflex II, Bruker, Billerica, MA) in linear positive (LP) mode to detect a mass range of 3,000 to 30,000 daltons and reflectron positive (RP) mode to detect a mass range of 500 to 5,000 daltons. The same samples analyzed by MS were also analyzed by tandem mass spectrometry (MS/MS) using the matrix assisted laser-desorption/ionization time-of-flight/time-of-flight (MALDI-TOF/TOF) technique in collision induced dissociation mode. FlexControl software (Bruker) was used to operate the spectrometer and flexAnalysis software (Bruker) was used to analyze and process the spectra.

Statistical Analysis

All statistics were performed using Graph Pad Prism 6 (GraphPad Software, La Jolla, CA). Data are represented as mean± SEM of results. To analyze RAGE and $A\beta_{1-42}$ binding to each of the neutrophil proteins with ELISAs, the optical density (OD) values were log transformed. Two-way analysis of variances (ANOVAs) were performed with Dunnett's multiple comparison tests. Student's unpaired *t* tests were performed to compare RAGE binding in the presence or absence of the RAGE antagonist, GM-0111 (values not in log). Kruskal-Wallis tests with Dunn's multiple comparison tests were used to analyze binding by Far-Western dot blotting (see figure legends 3 and 6 for details on multiple comparison tests). For analyzing $A\beta_{1-42}$ binding to RAGE with ELISAs, Kruskal Wallis tests were performed with Dunn's multiple comparisons test (see figure legends 4 and 5 for details on multiple comparison tests). To obtain dissociation constants (K_d), half-maximal inhibitory concentrations (IC_{50}), and maximum absorbance values, BSA was subtracted as background and values were fitted to a curve of nonlinear regression.

Results

CAP37 expression is highly correlated with ligands of RAGE

To determine the potential function of CAP37 in the brains of patients with AD, we first conducted an analysis to investigate which genes were within the "genetic neighborhood" of CAP37. GAMMA [11] was used to analyze transcriptomic data and identify genes highly correlated with CAP37. Then, protein-protein interactions between highly correlated genes were identified using the Human Proteome Reference Database. The subset of this network surrounding CAP37 (encoded by the gene *AZU1*) and *AGER* is shown in Fig 1. Green lines indicate the nature of the association is correlation, and black lines indicate protein-protein interactions. Genes that positively correlated with *AZU1* are represented by green boxes, and blue boxes represent protein-protein interactions between respective encoded genes. The genes encoding neutrophil proteins, neutrophil elastase (*ELANE*), cathepsin G (*CTSG*), and cathelicidin antimicrobial peptide (*CAMP*), positively correlated with *AZU1*. In addition, three of the S100-subtype calgranulin genes (*S100A12*, *S100A8*, and *S100A9*) correlated with *AZU1* (Fig 1). The S100 proteins are calcium binding proteins involved in various cell processes [27]. Similar to CAP37, these particular S100 proteins are expressed constitutively in neutrophils, mediate inflammatory responses, and have antimicrobial activities [27–29]. *AGER*, which encodes RAGE, was revealed by the Human Proteome Reference Database as one of the proteins interacting with S100A12. The literature indicates that S100A8, S100A9, and S100A12 are RAGE ligands that activate various cell responses by signaling through RAGE [27, 30]. Other proteins interacting with the S100 proteins included proteins involved in tumor suppression (*TP53*), transcriptional regulation (*LRIF1*), ubiquitination (*CACYBP*), and neurotransmitter release (*UNC119*). Due to the high correlation and functional similarities of CAP37 with the S100 proteins, we investigated whether CAP37 and two other neutrophil proteins, neutrophil elastase and cathepsin G, also interacted with RAGE.

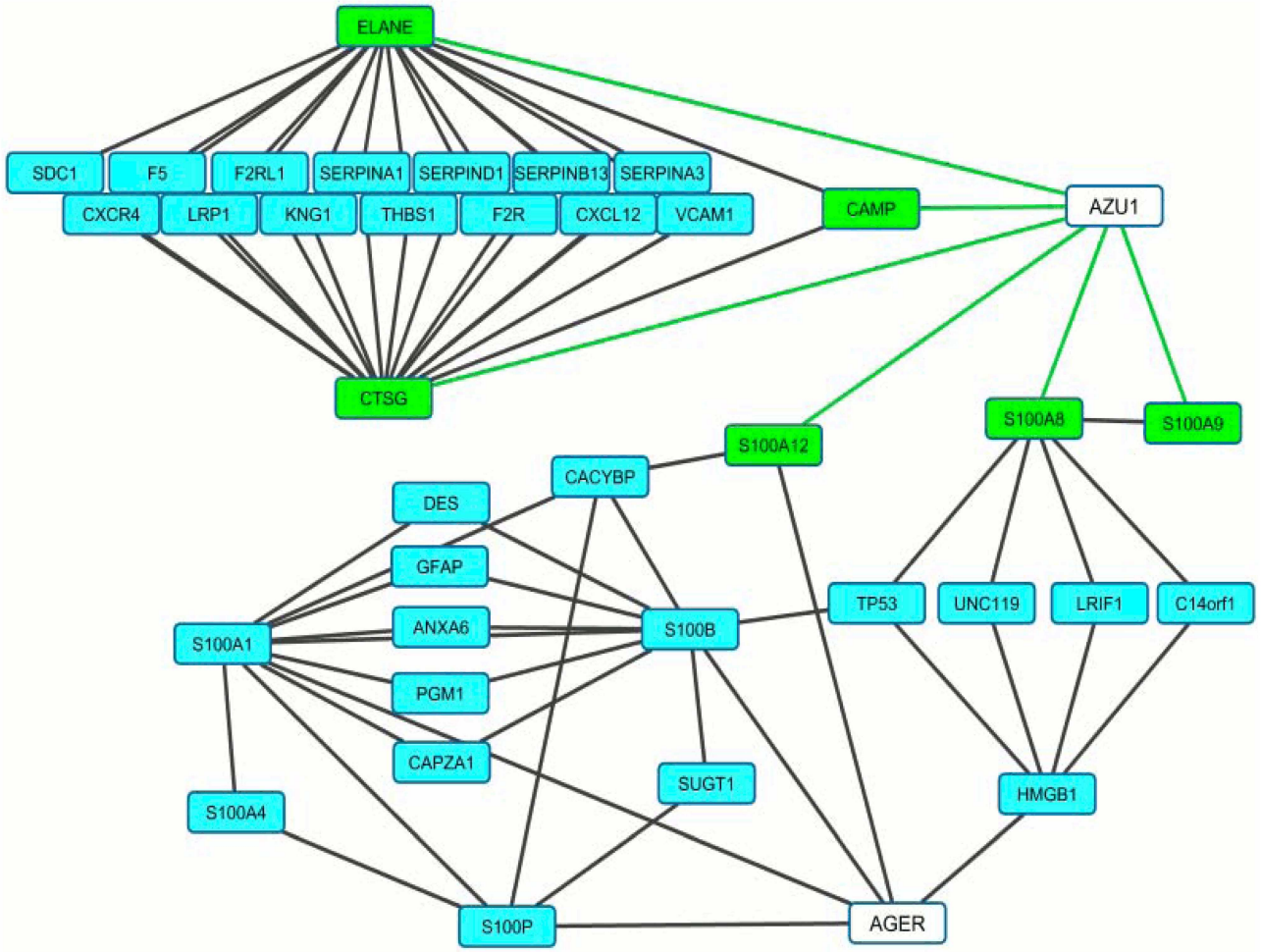

Fig 1. CAP37 expression is highly correlated with ligands of RAGE. Figure shows a network of genes correlated with *AZU1* (CAP37) and how they are associated with *AGER* (RAGE). Green lines indicate the nature of the association is correlation, and black lines indicate protein-protein interactions. Genes in green boxes are positively correlated with *AZU1*. Genes in blue boxes encode for proteins that interact with at least two other proteins in the network. Three of the genes shown in green boxes are S100 calgranulin genes (S100A8, S100A9, and S100A12), that encode for calcium binding proteins and are RAGE ligands. *S100A8*, *S100A9*, and *S100A12* correlated with *AZU1* with Pearson's correlation coefficient values (measures of linear correlations) of 0.41, 0.37, and 0.38, respectively. The expression of *ELANE* (neutrophil elastase), *CTSG* (cathepsin G), and *CAMP* (cathelicidin antimicrobial peptide) positively correlated with *AZU1* (Pearson's correlation coefficient values of 0.72, 0.62, and 0.43, respectively). Genes that positively correlated with *AZU1* had protein-protein interactions with genes involved in blood clotting (*F5*, *F2RL1*, *F2R*, *KNG1*), protease inhibition (*SERPIN*s), cell adhesion (*THBS1*, *SDC*, *VCAM1*), chemotaxis (*CXCR4*, *CXCL12*), Aβ transport (*LRP1*), and cytoskeletal structure (*CAPZA1*, *DES*, *GFAP*). A protein-protein interaction between *S100A12* and *AGER* is shown. Genes encoding for other ligands of RAGE (*S100B*, *S100P*, *S100A4*, *S100A1*) were also associated with *AZU1* based on the interactions in the network.

doi:10.1371/journal.pone.0163330.g001

RAGE binds specifically to CAP37, neutrophil elastase, and cathepsin G with different affinities

ELISAs were used to determine binding of RAGE to the neutrophil proteins CAP37, neutrophil elastase, and cathepsin G. RAGE was added at increasing concentrations to wells coated with the respective neutrophil proteins. The binding of RAGE to $A\beta_{1-42}$ was measured as a positive control since $A\beta_{1-42}$ is an established ligand of RAGE [14]. Binding of RAGE to BSA was measured as a control for non-specific protein binding. Dissociation constant (K_D) values, which indicate the protein concentration required to reach half-maximal binding at equilibrium and

reflect the binding affinity, were computed for binding of RAGE to each protein. The maximum absorbance values, which reflect the maximum number of binding sites, were also determined. Results demonstrated significantly more binding ($p<0.0001$) of RAGE to CAP37 than to BSA at all concentrations of RAGE tested (Fig 2a, Table 1). RAGE bound to CAP37 with a K_D value of 1.26 nM and a maximum absorbance value of 2.49 (Fig 2a, insert). Binding of RAGE to neutrophil elastase was also significantly higher ($p<0.01$) than binding to BSA, but only at the two highest concentrations of RAGE tested (Fig 2a, Table 1). A K_D value of 3.25 nM and a maximum absorbance value of 1.11 was computed for RAGE binding to neutrophil elastase (Fig 2a, insert). RAGE binding to cathepsin G was significantly higher ($p<0.0001$) than binding to BSA at all concentrations of RAGE tested (Fig 2a, Table 1), and a K_D value of 0.45 nM and a maximum absorbance value of 2.14 were obtained (Fig 2a, insert). Among the three neutrophil proteins, CAP37 bound to the highest number of RAGE molecules (based on maximum absorbance values). RAGE binding to cathepsin G exhibited the lowest K_D value and hence the highest affinity. As expected, results showed significantly higher binding ($p<0.0001$) of RAGE to $A\beta_{1-42}$ compared to BSA at all concentrations of RAGE tested (Fig 2a, Table 1). A K_D value of 3.97 nM and maximum absorbance value of 5.65 was calculated for RAGE binding to $A\beta_{1-42}$ (Fig 2a, insert).

To determine whether or not binding of RAGE to the neutrophil proteins could be inhibited by a specific inhibitor of RAGE, we measured binding of RAGE to the neutrophil proteins in the presence of the RAGE antagonist, GM-0111. When GM-0111 was pre-incubated with RAGE, binding of RAGE to CAP37 was significantly reduced (Fig 2b, Table 2B). Pre-incubation with GM-0111 also significantly reduced the binding of RAGE to neutrophil elastase, but binding was only reduced when the highest concentration of RAGE was added (Fig 2b, Table 2B). Although binding of RAGE to cathepsin G was observed with high affinity, pre-incubation of RAGE with GM-0111 did not significantly reduce binding of RAGE to cathepsin G (Fig 2b, Table 2B). As would be expected, GM-0111 significantly reduced the binding of RAGE to $A\beta_{1-42}$ but not to BSA (Fig 2b, Table 2A).

Far Western dot blot analysis was used to confirm the binding of RAGE to neutrophil proteins. Similar to results obtained with ELISAs, far-Western dot blot analysis demonstrated strong binding of RAGE to $A\beta_{1-42}$ and CAP37 (Fig 3a). Binding of RAGE to cathepsin G was also observed. However, binding of RAGE to cathepsin G was not significantly higher than RAGE binding to BSA. We did not detect visible binding of RAGE to neutrophil elastase or BSA using this approach. These results are congruent with ELISA results, which also showed the lowest binding of RAGE to neutrophil elastase and BSA. Mean dot density quantification using Image J software revealed that binding of RAGE to $A\beta_{1-42}$ and CAP37 was significantly higher than binding of RAGE to BSA (Fig 3b). Similar to ELISAs, GM-0111 also significantly decreased the binding of RAGE to $A\beta_{1-42}$ and CAP37 in far-Western dot blot experiments (Fig 3c).

CAP37 and neutrophil elastase decrease the amyloid beta-RAGE interaction by distinct mechanisms

Upon observing that the binding of CAP37, neutrophil elastase, and $A\beta_{1-42}$ to RAGE could be inhibited by the antagonist, GM-0111, we next sought to determine if either CAP37 or neutrophil elastase could compete with $A\beta_{1-42}$ for the same binding site on RAGE. Results obtained from ELISAs, demonstrated that when $A\beta_{1-42}$ and CAP37 were added simultaneously to wells containing RAGE, CAP37 significantly decreased the binding of $A\beta_{1-42}$ to RAGE in a dose-dependent manner (Fig 4a). CAP37 inhibited the binding of $A\beta_{1-42}$ to RAGE with a half maximal inhibitory concentration (IC_{50}) value of 1.28 μM. Under these conditions, the concentration of CAP37 (1.28 μM) is ≈ 100-fold higher than the concentration of $A\beta_{1-42}$ (11 nM).

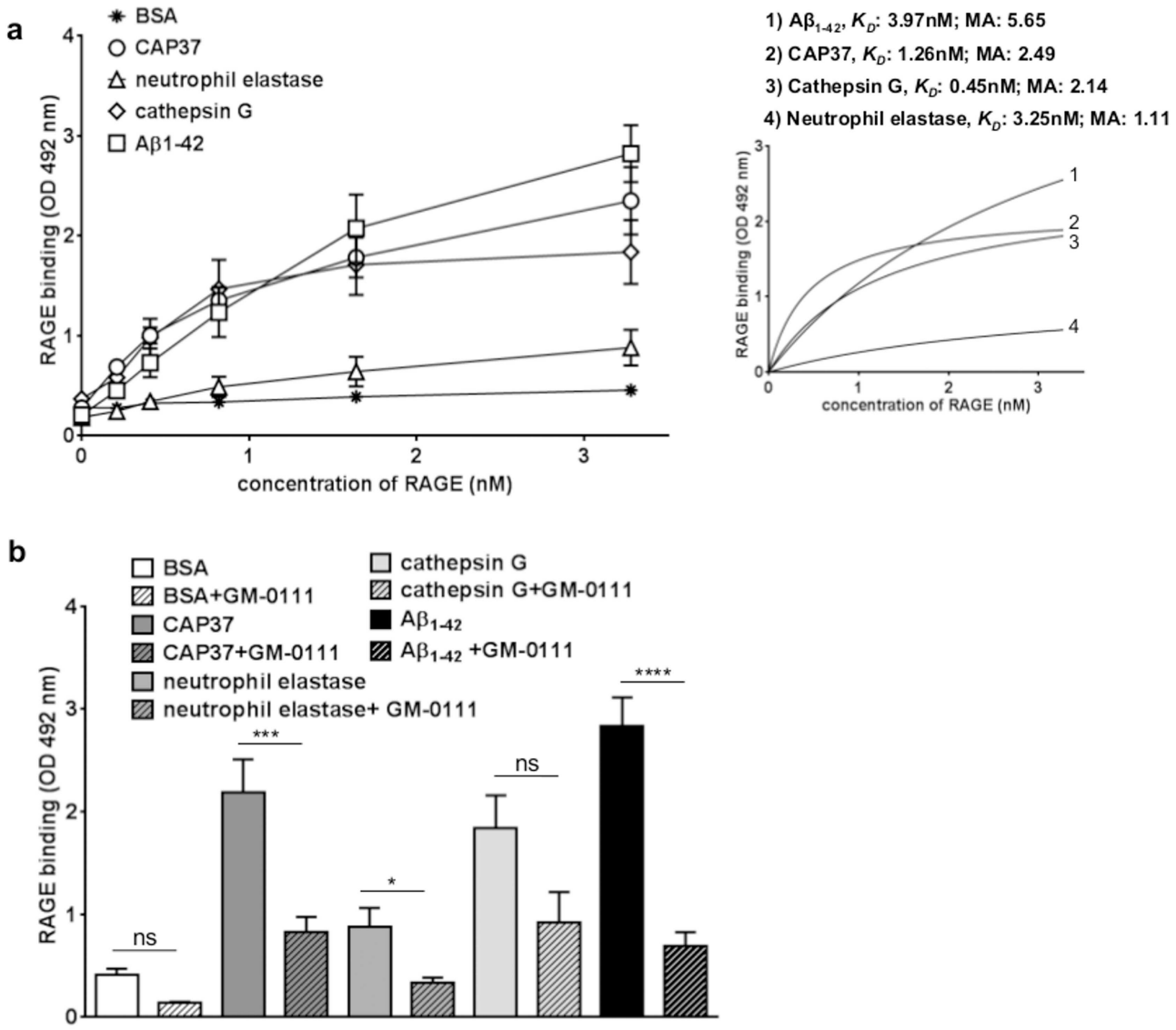

Fig 2. RAGE binds specifically to CAP37, neutrophil elastase, and cathepsin G, but with different affinities. (a) Graph shows the binding of RAGE to BSA (stars), CAP37 (circles), neutrophil elastase (triangles), cathepsin G (diamonds), and $A\beta_{1-42}$(squares). BSA: n = 20, CAP37: n = 11, neutrophil elastase: n = 7, cathepsin G: n = 9, $A\beta_{1-42}$: n = 12. Data are mean ± SEM of results. K_D values and maximum absorbance (MA) values were obtained after subtracting BSA as background and fitting values to curves of nonlinear regression (see insert). (b) Graph shows binding of RAGE (3.3 nM) to BSA (white bars), CAP37 (dark gray bars), neutrophil elastase (medium gray bars), cathepsin G (light gray bars), and $A\beta_{1-42}$(black bars) after pre-incubating in the absence (solid bars) or presence (striped bars) of GM-0111. BSA: n = 20, BSA+GM-0111: n = 3, CAP37: n = 11, CAP37+GM-0111: n = 10, neutrophil elastase: n = 7, neutrophil elastase+GM-0111: n = 6, cathepsin G: n = 9, cathepsin G+GM-0111: n = 4, $A\beta_{1-42}$: n = 12, $A\beta_{1-42}$ +GM-0111: n = 9. Student's unpaired *t* tests were performed to compare binding of RAGE to each protein in the presence and absence of GM-0111. Data are mean ± SEM of results. *p<0.05,***p<0.001, ****p<0.0001 when comparing binding with and without GM-0111.

doi:10.1371/journal.pone.0163330.g002

Neutrophil elastase significantly decreased the binding of $A\beta_{1-42}$ to RAGE with a very low IC_{50} value of 4.58 nM (Fig 4b). Since we did not observe strong binding of RAGE to neutrophil elastase (Fig 2a), inhibition by neutrophil elastase with such a low IC_{50} value led us to question if this inhibition was indeed due to displacement of $A\beta_{1-42}$ binding to RAGE or if it may have been due to the proteolytic activity of neutrophil elastase. To determine this, we measured binding and inhibition of the $A\beta_{1-42}$- RAGE interaction in the presence of a protease inhibitor

Table 1. RAGE binding to $A\beta_{1-42}$, CAP37, neutrophil elastase, and cathepsin G.

RAGE (nM)	Log binding			
	$A\beta_{1-42}$	CAP37	Neutrophil elastase	Cathepsin G
0	• -0.726±0.054 ns • p = 0.851	• -0.623±0.077 ns • p = 0.979	• -0.756±0.060 ns • p = 0.744	• -0.426±0.058 ns • p = 0.105
0.21	• -0.387±0.058* • p = 0.011	• -0.174±0.031**** • p<0.0001	• -0.629±0.055 ns • p = 0.10	• -0.264±0.062*** • p = 0.0002
0.42	• -0.214±0.076**** • p<0.0001	• -0.012±0.034**** • p<0.0001	• -0.510±0.087 ns • p = 0.859	• -0.078±0.0089**** • p<0.0001
0.83	• -0.013±0.094**** • p<0.0001	• 0.112±0.041**** • p<0.0001	• -0.376±0.101 ns • p = 0.136	• 0.101±0.084**** • p<0.0001
1.67	• 0.238±0.088**** • p<0.0001	• 0.228±0.043**** • p<0.0001	• -0.274±0.113* • p = 0.046	• 0.166±0.092**** • p<0.0001
3.33	• 0.425±0.048**** • p<0.0001	• 0.325±0.064**** • p<0.0001	• -0.121±0.104** • p = 0.003	• 0.192±0.096**** • p<0.0001

Log RAGE binding is shown as mean± SEM. A two-way ANOVA was performed with Dunnett's multiple comparisons test so that binding of RAGE to each protein was compared to binding of RAGE to BSA.

*p<0.05

**p<0.01

***p<0.001

****p<0.0001

doi:10.1371/journal.pone.0163330.t001

cocktail. Interestingly, addition of protease inhibitors completely prevented neutrophil elastase from inhibiting $A\beta_{1-42}$ binding to RAGE (Fig 4b). This indicated that neutrophil elastase was not likely competitively displacing $A\beta_{1-42}$ bound to RAGE, but was more likely degrading the $A\beta_{1-42}$ to prevent it from binding to RAGE. The protease inhibitors did not prevent CAP37 from inhibiting the $A\beta_{1-42}$-RAGE interaction (Fig 4a). However, maximal inhibition in the absence of protease inhibitors was complete (no Aβ binding to RAGE at the highest dose of CAP37), and only partial in the presence of protease inhibitors. This raised the possibility that CAP37 also had some enzymatic activity against $A\beta_{1-42}$, although most likely less potent compared to neutrophil elastase.

Based on these findings, we next questioned whether the $A\beta_{1-42}$-RAGE interaction could be disrupted through direct interactions of the neutrophil proteins with $A\beta_{1-42}$. To determine this, we performed ELISAs in which CAP37 and neutrophil elastase were pre-incubated with $A\beta_{1-42}$ before adding $A\beta_{1-42}$ to wells containing RAGE. Interestingly, when pre-incubated with $A\beta_{1-42}$, both CAP37 (Fig 5a) and neutrophil elastase (Fig 5b) significantly reduced the interaction of $A\beta_{1-42}$ with RAGE in a dose dependent manner. CAP37 (at 2 μg/ml) increased the K_D value for $A\beta_{1-42}$ binding to RAGE from 6.64 nM to 148.70 nM (Fig 5a, insert) but did not change the maximum absorbance value (3.24 to 3.27 OD 492 nm), whereas, neutrophil elastase (at 2 μg/ml) increased the K_D value from 5.21 nM to 130.90 nM (Fig 5b, insert) and reduced the maximum absorbance value (3.54 to 0.15 OD 492 nm). This indicates that CAP37 and neutrophil elastase likely inhibit the interaction of $A\beta_{1-42}$ with RAGE through distinct mechanisms, and the results suggest two mechanisms of inhibition were possible. CAP37 and neutrophil elastase could be proteolytically degrading the $A\beta_{1-42}$, preventing it from binding to RAGE. Alternatively, CAP37 and neutrophil elastase could be binding $A\beta_{1-42}$ with a high affinity, and therefore, sequestering it away from RAGE.

Table 2. Inhibition of RAGE binding BSA, $A\beta_{1-42}$, CAP37, neutrophil elastase, and cathepsin G with GM0-111.

A

RAGE (nM)	BSA		$A\beta_{1-42}$	
	RAGE binding (OD 492 nm)		RAGE binding (OD 492 nm)	
	-GM-0111	+GM-0111	-GM-0111	+GM-0111
0	0.260±0.044	• 0.117±0.006 ns • p = 0.229	0.208±0.034	• 0.190±0.021 ns • p = 0.690
0.21	0.255±0.030	• 0.125±0.013 ns • p = 0.109	0.451±0.057	• 0.284±0.040 * • p = 0.038
0.42	0.296±0.036	• 0.128±0.013 ns • p = 0.092	0.730±0.144	• 0.339±0.052 * • p = 0.036
0.83	0.307±0.044	• 0.127±0.015 ns • p = 0.137	1.234±0.247	• 0.448±0.072 * • p = 0.015
1.67	0.350±0.046	• 0.151±0.018 ns • p = 0.118	2.086±0.335	• 0.540±0.091 *** • p = 0.0009
3.33	0.412±0.057	• 0.138±0.008 ns • p = 0.082	2.834±0.275	• 0.693±0.133 **** • p<0.0001

B

RAGE (nM)	CAP37		Neutrophil elastase		Cathepsin G	
	RAGE binding (OD 492 nm)		RAGE binding (OD 492 nm)		RAGE binding (OD 492 nm)	
	-GM-0111	+GM-0111	-GM-0111	+GM-0111	-GM-0111	+GM-0111
0	0.277±0.047	• 0.340±0.079 ns • p = 0.499	0.183± 0.019	• 0.183±0.021 ns • p = 0.972	0.369 ±0.043	• 0.489±0.101 ns • p = 0.214
0.21	0.688±0.052	• 0.355±0.042 **** • p<0.0001	0.246± 0.027	• 0.187±0.024 ns • p = 0.137	0.583 ±0.065	• 0.461±0.067 ns • p = 0.283
0.42	1.002±0.082	• 0.409±0.051 **** • p<0.0001	0.343±0.055	• 0.208±0.029 ns • p = 0.063	0.979 ±0.192	• 0.586±0.104 ns • p = 0.220
0.83	1.353±0.134	• 0.563±0.076 **** • p<0.0001	0.488±0.100	• 0.254±0.036 ns • p = 0.065	1.467 ±0.293	• 0.839±0.181 ns • p = 0.204
1.67	1.783±0.201	• 0.648±0.111 *** • p = 0.0001	0.641±0.148	• 0.294±0.041 ns • p = 0.059	1.709 ±0.302	• 0.942±0.241 ns • p = 0.145
3.33	2.349±0.338	• 0.826±0.146 *** • p = 0.0007	0.882±0.179	• 0.332±0.050 * • p = 0.019	1.838 ±0.320	• 0.924±0.292 ns • p = 0.109

RAGE binding is shown as mean± SEM. Student's unpaired *t* tests were performed to compare RAGE binding in the presence or absence of RAGE antagonist, GM-0111.

*p<0.05

**p<0.01

***p<0.001

****p<0.0001

doi:10.1371/journal.pone.0163330.t002

$A\beta_{1-42}$ binds to CAP37, neutrophil elastase, and cathepsin G with different affinities

To explore the possibility that neutrophil proteins could bind and sequester $A\beta_{1-42}$, we tested for specific binding of $A\beta_{1-42}$ to CAP37, neutrophil elastase, or cathepsin G. This was achieved by performing an ELISA in which $A\beta_{1-42}$ was added at increasing concentrations to wells containing 500 ng of CAP37, neutrophil elastase, or cathepsin G. This experiment was performed

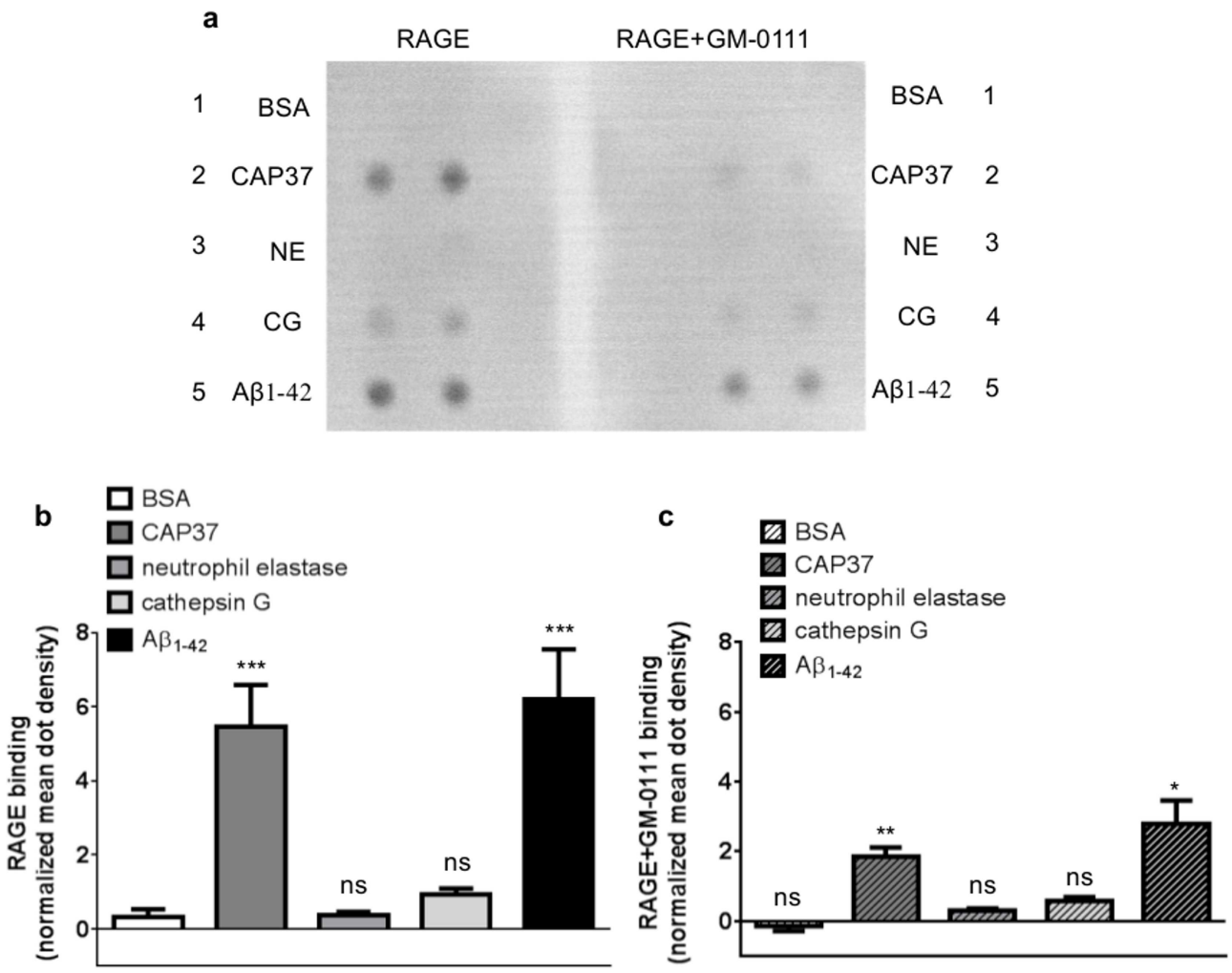

Fig 3. Far-Western dot blotting confirms the binding of RAGE to neutrophil proteins and inhibition of binding with GM-0111. (a) Far-Western dot blots show the binding of RAGE to BSA (row 1), CAP37 (row 2), neutrophil elastase (NE, row 3), cathepsin G (CG, row 4), and $A\beta_{1-42}$ (row 5) when RAGE was pre-incubated in the absence (left) or presence (right) of the RAGE inhibitor, GM-0111. Proteins were spotted in duplicate on each blot. (b) Histogram quantification of RAGE binding to BSA, CAP37, neutrophil elastase, cathepsin G, and $A\beta_{1-42}$ is represented by the white bar, dark gray bar, medium gray bar, light gray bar, and black bar, respectively. BSA: n = 9, CAP37: n = 9, neutrophil elastase: n = 6, cathepsin G: n = 6, $A\beta_{1-42}$: n = 8. Data are mean ± SEM of results. Mean dot densities were normalized to the mean dot densities of ponceau S staining for each dot. A Kruskal-Wallis test was performed with Dunn's multiple comparisons test to compare the binding of RAGE to each neutrophil protein with the binding of RAGE to BSA. (c) Histogram quantification of RAGE (pre-incubated with GM-0111) binding to BSA, CAP37, neutrophil elastase, cathepsin G, and $A\beta_{1-42}$ is represented by the striped white bar, striped dark gray bar, striped medium gray bar, striped light gray bar, and striped black bar, respectively. BSA+GM-0111: n = 8, CAP37 +GM-0111: n = 8, neutrophil elastase+GM-0111: n = 5, cathepsin G+GM-0111: n = 5, $A\beta_{1-42}$+GM-0111: n = 7. Data are mean ± SEM of results. Mean dot densities were normalized to the mean dot densities of ponceau S staining for each dot. Asterisks (*) indicate significant results from student's unpaired *t* tests, which were used to compare binding of RAGE to each protein in the absence and presence of GM-0111.

doi:10.1371/journal.pone.0163330.g003

in the presence of protease inhibitors to establish binding in absence of proteolytic activity. Binding of $A\beta_{1-42}$ to BSA was measured as a control for non-specific protein binding. We observed binding of $A\beta_{1-42}$ to all three neutrophil proteins; we observed significantly higher ($p<0.01$ to $p<0.0001$) binding of $A\beta_{1-42}$ to CAP37 compared to BSA at all doses of $A\beta_{1-42}$ tested (Fig 6, Table 3). $A\beta_{1-42}$ bound to CAP37 with a calculated K_D value of 37.92 nM and a maximum absorbance value of 2.86 (Fig 6, insert). Binding of $A\beta_{1-42}$ to cathepsin G was also significantly higher than binding to BSA at all concentrations of $A\beta_{1-42}$ (Fig 6, Table 3). An

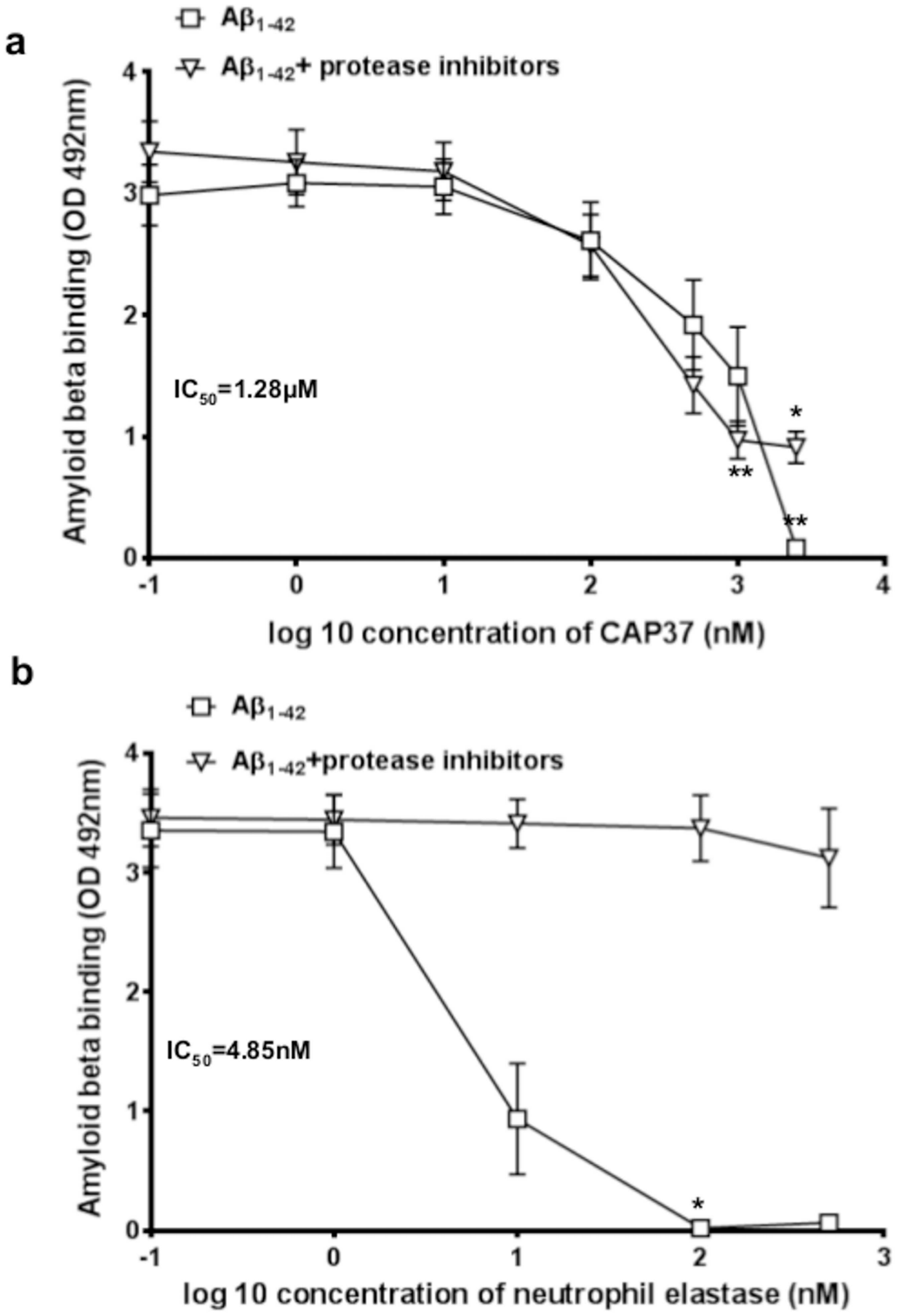

Fig 4. Neutrophil proteins inhibit $A\beta_{1-42}$ binding to RAGE. (a) Graph shows binding of $A\beta_{1-42}$ to RAGE when CAP37 was added simultaneously to wells at increasing concentrations in the presence (inverted triangles) or absence (squares) of protease inhibitors. An IC_{50} value of 1.28 μM was computed for inhibition of $A\beta_{1-42}$ binding to RAGE by CAP37. Two separate Kruskal-Wallis tests were performed for $A\beta_{1-42}$ binding in the presence and absence of protease inhibitors. A Dunn's multiple comparisons test was performed for each separate Kruskal-Wallis test to compare binding of $A\beta_{1-42}$ to RAGE in the presence of increasing

concentrations of CAP37. Data are mean ± SEM of results. *p<0.05, **p<0.01. (b) Graph shows binding of $A\beta_{1-42}$ to RAGE when neutrophil elastase was added simultaneously to wells at increasing concentrations in the presence (inverted triangles) or absence (squares) of protease inhibitors. An IC_{50} value of 4.85 nM was computed for inhibition of $A\beta_{1-42}$ binding to RAGE by neutrophil elastase in the absence of protease inhibitors. Two separate Kruskal-Wallis tests were performed for $A\beta_{1-42}$ binding in the presence and absence of protease inhibitors. A Dunn's multiple comparisons test was performed for each separate Kruskal-Wallis test to compare binding of $A\beta_{1-42}$ to RAGE in the presence of increasing concentrations of neutrophil elastase. No inhibition occurred in the presence of protease inhibitors. Data are mean ± SEM of results. *p<0.05.

doi:10.1371/journal.pone.0163330.g004

absorbance background, likely due to a non-specific reaction between the antibody for $A\beta_{1-42}$ and CAP37 and cathepsin G was observed in the absence of $A\beta_{1-42}$ (Table 3). A K_D value of 20.71 nM and maximum absorbance value of 3.54 was computed for $A\beta_{1-42}$ binding to cathepsin G (Fig 6, insert). Binding of $A\beta_{1-42}$ to neutrophil elastase (Fig 6, Table 3) was lower, but was significant starting at an $A\beta_{1-42}$ concentration of 6.93 nM. A higher K_D value of 470.80 nM and a maximum absorbance value of 5.89 was computed for $A\beta_{1-42}$ binding to neutrophil elastase (Fig 6, insert).

Far-Western dot blot analysis was used to confirm the binding of $A\beta_{1-42}$ to neutrophil proteins. Similar to results obtained with ELISAs, far-Western dot blot analysis demonstrated strong binding of $A\beta_{1-42}$ to CAP37 and cathepsin G and low binding to neutrophil elastase (Fig 6b). No binding of $A\beta_{1-42}$ to BSA was visible. Mean dot density quantification using Image J software revealed that binding of $A\beta_{1-42}$ to CAP37 and cathepsin G was significantly higher than binding of $A\beta_{1-42}$ to BSA (Fig 6c). However, binding of $A\beta_{1-42}$ to neutrophil elastase was not significantly higher than binding of $A\beta_{1-42}$ to BSA.

CAP37, neutrophil elastase, and cathepsin G cleave $A\beta_{1-42}$

Our results suggest that neutrophil proteins could inhibit the binding of $A\beta_{1-42}$ to RAGE through direct binding and sequestering of $A\beta_{1-42}$. We also observed that enzymatic degradation of $A\beta_{1-42}$ could be inhibited by protease inhibitors, but without the inhibitors, the $A\beta_{1-42}$ was degraded and binding to RAGE eliminated. In this experiment, we aimed to establish unequivocally the cleavage of $A\beta_{1-42}$. We performed MALDI-TOF MS on Aβ that was incubated with CAP37 (Fig 7) in the presence and absence of protease inhibitors at room temperature up to 5 h (t≈0.25 min to t = 300 min), or with neutrophil elastase (Fig 8) or cathepsin G (Fig 9) at room temperature for up to 1 h (t≈0.25 m to t = 60 min). Proteins were incubated at room temperature rather than 37°C due to the formation of $A\beta_{1-42}$ aggregates at 37°C. Immediately after adding CAP37 (t≈0.25 min), we observed a peak at 4500 Da corresponding to the full length $A\beta_{1-42}$ (Fig 7a), which represented 76.65% of the total intensity (Fig 7c) of Aβ peaks (intact full peptide + fragments generated). As shown in Fig 7b, after $A\beta_{1-42}$ incubated for 210 min with CAP37, the 4500 Da peak was smaller than when amyloid beta incubated alone or incubated with CAP37 in the presence of protease inhibitors. In addition, two large peaks appeared at 3616 Da and 3505 Da after incubation with CAP37, which were not present when $A\beta_{1-42}$ was incubated alone or with CAP37 and protease inhibitors. No peaks corresponding to the molecular weight of $A\beta_{1-42}$ or the products of $A\beta_{1-42}$ appeared when CAP37 was incubated alone. The percent peak intensity for the full peptide gradually decreased and percent peak intensities for the fragment products increased with increasing incubation time in the presence of CAP37 (Fig 7c).

Incubation of $A\beta_{1-42}$ with neutrophil elastase resulted in a rapid degradation of $A\beta_{1-42}$. Immediately after the addition of neutrophil elastase (t≈0.25 min), the full $A\beta_{1-42}$ peak was reduced to 28.83% (Fig 8c) and two fragment peaks were evident at 3616 Da and 3505 Da (Fig 8a). Five additional products (2877 Da, 2168 Da, 2069 Da, 1425 Da, and 1355 Da) predicted to

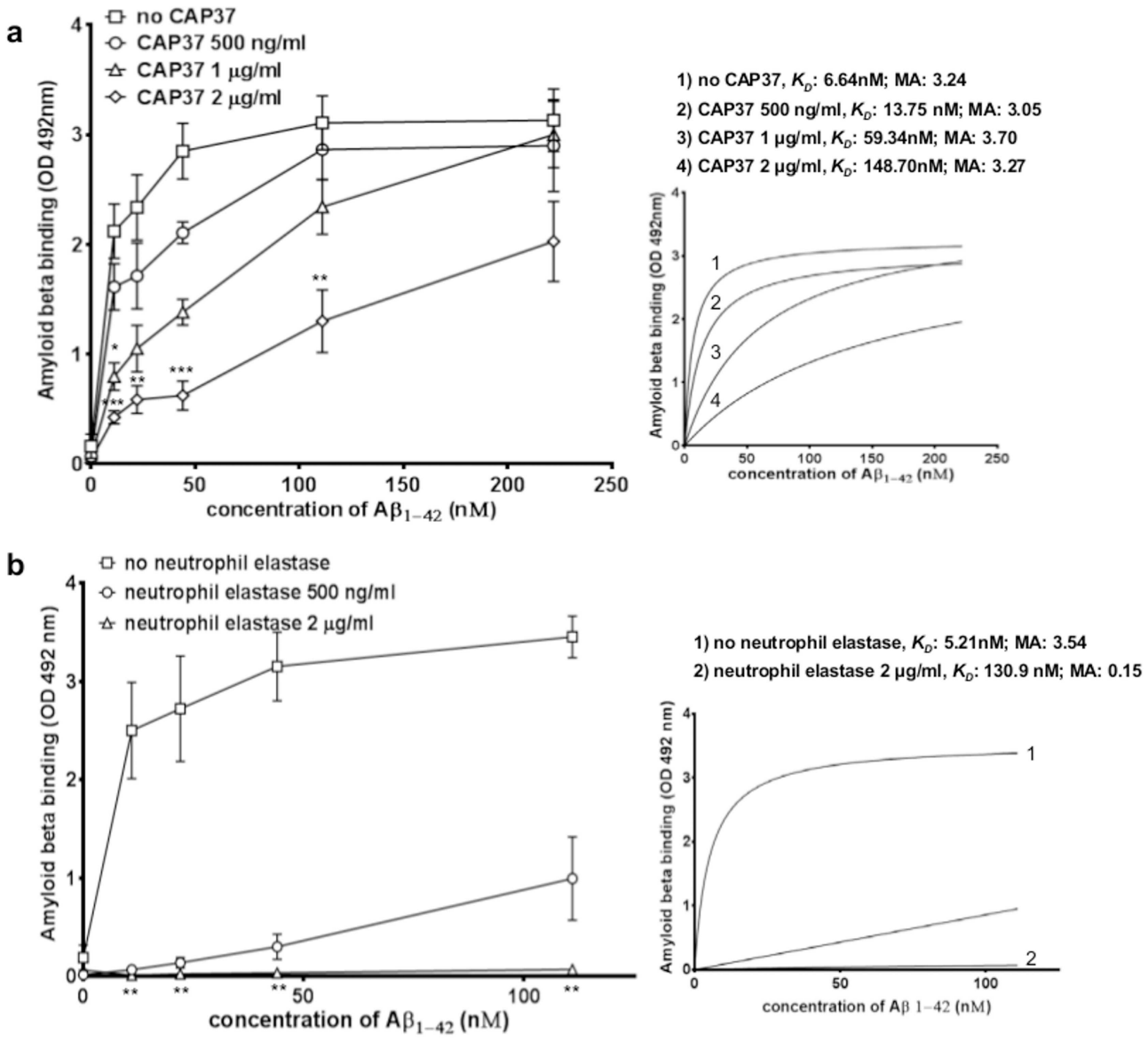

Fig 5. Neutrophil proteins pre-incubated with $A\beta_{1-42}$ inhibit the binding of $A\beta_{1-42}$ to RAGE. (a) Graph shows binding of $A\beta_{1-42}$ to RAGE when $A\beta_{1-42}$ was pre-incubated alone (squares) and a dose-dependent reduction of $A\beta_{1-42}$ binding to RAGE when $A\beta_{1-42}$ pre-incubated with 0.5 μg/ml (21 nM, circles), 1 μg/ml (42 nM, triangles), or 2 μg/ml CAP37 (83 nM, diamonds). No CAP37: n = 5, +CAP37 0.5 μg/ml: n = 3, +CAP37 1 μg/ml: n = 4, +CAP37 2 μg/ml: n = 4. BSA was subtracted as background from all curves. Separate Kruskal-Wallis tests were performed to analyze binding at each concentration of $A\beta_{1-42}$. A Dunn's multiple comparisons test was performed for each Kruskal-Wallis test to compare binding of $A\beta_{1-42}$ to RAGE when $A\beta_{1-42}$ pre-incubated with increasing concentrations of CAP37. *p<0.05, **p<0.01, ***p<0.001. K_D values and maximum absorbance (MA) values were computed after fitting values to curves of nonlinear regression (see insert). (b) Graph shows binding of $A\beta_{1-42}$ to RAGE when $A\beta_{1-42}$ pre-incubated alone (squares) and a dose-dependent reduction of the $A\beta_{1-42}$ binding RAGE when $A\beta_{1-42}$ pre-incubated with 0.5 μg/ml (20 nM, circles) or 2 μg/ml neutrophil elastase (80 nM, triangles). No neutrophil elastase: n = 5, +neutrophil elastase 0.5 μg/ml: n = 4, +neutrophil elastase 2 μg/ml: n = 5. BSA was subtracted as background from all curves. Separate Kruskal-Wallis tests were performed to analyze binding at each concentration of $A\beta_{1-42}$. A Dunn's multiple comparisons test was performed for each Kruskal-Wallis test to compare binding of $A\beta_{1-42}$ to RAGE when $A\beta_{1-42}$ pre-incubated with increasing concentrations of neutrophil elastase.**p<0.01. K_D values and maximum absorbance (MA) were computed after fitting values to curves of nonlinear regression (see insert).

doi:10.1371/journal.pone.0163330.g005

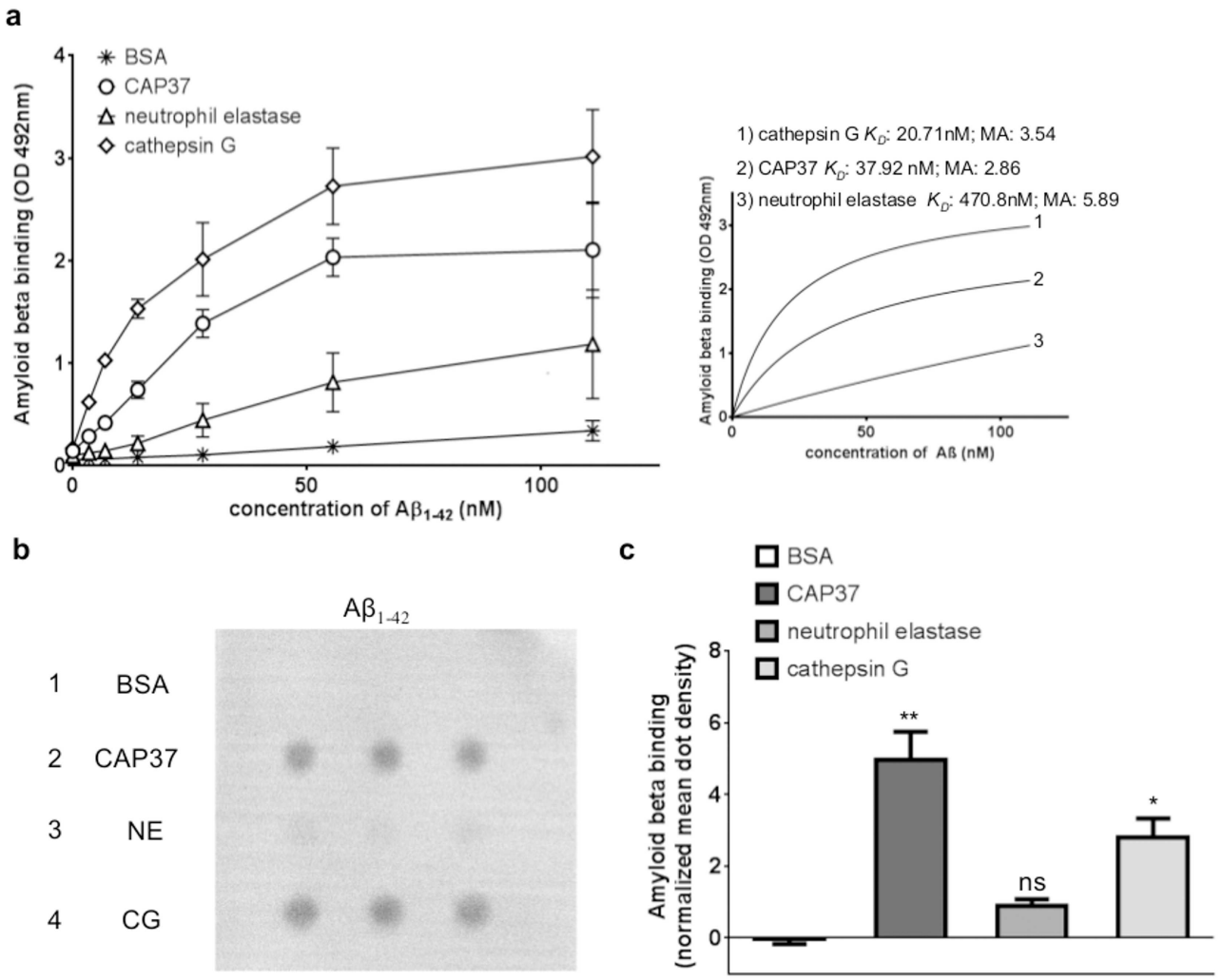

Fig 6. Amyloid beta binds to CAP37, neutrophil elastase, and cathepsin G with different affinities. (a) Graph shows binding of $A\beta_{1-42}$ to CAP37 (circles), neutrophil elastase (triangles), cathepsin G (diamonds), and BSA (stars). n = 3 for all proteins. Data are mean ± SEM of results. K_D values and maximum absorbance (MA) values were obtained after subtracting BSA as background and fitting values to curves of nonlinear regression (see insert). (b) Far-Western dot blot shows the binding of $A\beta_{1-42}$ to BSA (row 1), CAP37 (row 2), neutrophil elastase (NE, row 3), and cathepsin G (CG, row 4). Proteins were spotted in triplicate across each row. (c) Histogram quantification of $A\beta_{1-42}$ binding BSA, CAP37, neutrophil elastase, and cathepsin G, represented by the white bar, dark gray bar, medium gray bar, and light gray bar, respectively. n = 4 for all proteins. Data are mean ± SEM of results. Mean dot densities were normalized to the mean dot densities of ponceau S staining for each dot. A Kruskal-Wallis test was performed with Dunn's multiple comparisons test to compare the binding of $A\beta_{1-42}$ to each neutrophil protein with the binding of $A\beta_{1-42}$ to BSA. *p<0.05, **p<0.01.

doi:10.1371/journal.pone.0163330.g006

be degraded $A\beta_{1-42}$ were observed after incubation with neutrophil elastase for 60 min (Fig 8b). No peaks corresponding to the molecular mass of $A\beta_{1-42}$ or the products of $A\beta_{1-42}$ appeared when neutrophil elastase was incubated alone. The percent peak intensity of $A\beta_{1-42}$ decreased from 28.83% to <1% by t = 5 min (Fig 8c). Percent peak intensities for the largest products that were generated (3616 Da and 3505 Da) decreased with increasing incubation time. For medium sized products (2877 Da, 2168 Da, and 2069 Da), percent peak intensities first increased at early time points, and then decreased with longer incubation time. The percent peak intensities for the smallest products observed (1425 Da and 1355 Da) appeared at t = 5 min incubation time with neutrophil elastase and gradually increased with increasing incubation time.

Table 3. $A\beta_{1-42}$ binding to CAP37, neutrophil elastase, and cathepsin G.

$A\beta_{1-42}$ (nM)	Log binding		
	CAP37	Neutrophil elastase	Cathepsin G
0	• -0.907±0.139** • p = 0.005	• -1.061±0.114 ns • p = 0.119	• -0.884±0.103 *** • p = 0.0004
3.47	• -0.556±0.047 **** • p<0.0001	• -0.961±0.139 ns • p = 0.169	• -0.368±0.157 **** • p<0.0001
6.93	• -0.389±0.051 **** • p<0.0001	• -0.890±0.127 * • p = 0.0064	• -0.152±0.162 **** • p<0.0001
13.89	• -0.138±0.047 **** • p<0.0001	• -0.720±0.151 ** • p = 0.0064	• 0.019±0.165 **** • p<0.0001
27.78	• 0.137±0.043 **** • p<0.0001	• -0.414±0.154 **** • p<0.0001	• 0.151±0.149 **** • p<0.0001
55.56	• 0.304±0.039 **** • p<0.0001	• -0.146±0.153 **** • p<0.0001	• 0.310±0.125 **** • p<0.0001
111	• 0.377±0.075 **** • p<0.0001	• 0.123±0.176 *** • p = 0.0004	• 0.541±0.002 **** • p<0.0001

Log $A\beta_{1-42}$ binding is shown as mean± SEM. A two-way ANOVA was performed with Dunnett's multiple comparisons test so that binding of $A\beta_{1-42}$ to each protein was compared to binding of $A\beta_{1-42}$ to BSA.

*p<0.05

**p<0.01

***p<0.001

****p<0.0001

doi:10.1371/journal.pone.0163330.t003

$A\beta_{1-42}$ that was incubated with cathepsin G was also rapidly degraded. Immediately after adding cathepsin G (t≈0.25 min), the full-length $A\beta_{1-42}$ peak represented only 27.43% of the total $A\beta_{1-42}$ (Fig 9c) and three additional peaks predicted to be fragments of $A\beta_{1-42}$ were present (Fig 9a, 2072 Da, 2001 Da, 1844 Da). The large peak appearing at 2464 Da was identified by MALDI TOF MS/MS as cathepsin G (data not shown). An additional fragment at 1476 Da was observed after $A\beta_{1-42}$ incubation with cathepsin G for 5 min (Fig 9b and 9c). No peaks corresponding to the mass of $A\beta_{1-42}$ or the products of $A\beta_{1-42}$ appeared when cathepsin G was incubated alone. $A\beta_{1-42}$ was completely degraded by t = 5 min (Fig 9c). The percent peak intensity for the largest product (2072 Da) gradually decreased with increasing incubation time. For medium sized fragments (2001 Da and 1844 Da), percent peak intensities first increased with early incubation time, and then decreased with longer incubation time. The percent peak intensity for the smallest product observed (1476 Da) appeared at t = 5 min incubation with cathepsin G and gradually increased with increasing incubation time.

MALDI TOF MS/MS was used to determine the sequences of the resultant fragment peaks generated by CAP37, neutrophil elastase, and cathepsin G. Products at 3616 Da and 3505 Da that were generated by CAP37 were identified as $A\beta_{1-32}$ and $A\beta_{1-31}$ (Table 4), with cleavage sites between Ile^{31} and Ile^{32} and between $Ile^{32}$and Gly^{33} (Fig 10a). CAP37, therefore, cleaved $A\beta_{1-42}$ within its C-terminal region. $A\beta_{1-42}$ products at 3616 Da and 3505 Da that were generated by neutrophil elastase were the same as those generated by CAP37 (Table 4). Therefore, $A\beta_{1-42}$ was also cleaved at Ile^{31}-Ile^{32} and Ile^{32}-Gly^{33} by neutrophil elastase (Fig 10b). Products at 2877 Da and 1425 Da cleaved by neutrophil elastase were identified as $A\beta_{1-24}$ and $A\beta_{1-12}$. We were unable to identify the product at 2168 Da with MS/MS, and we have predicted

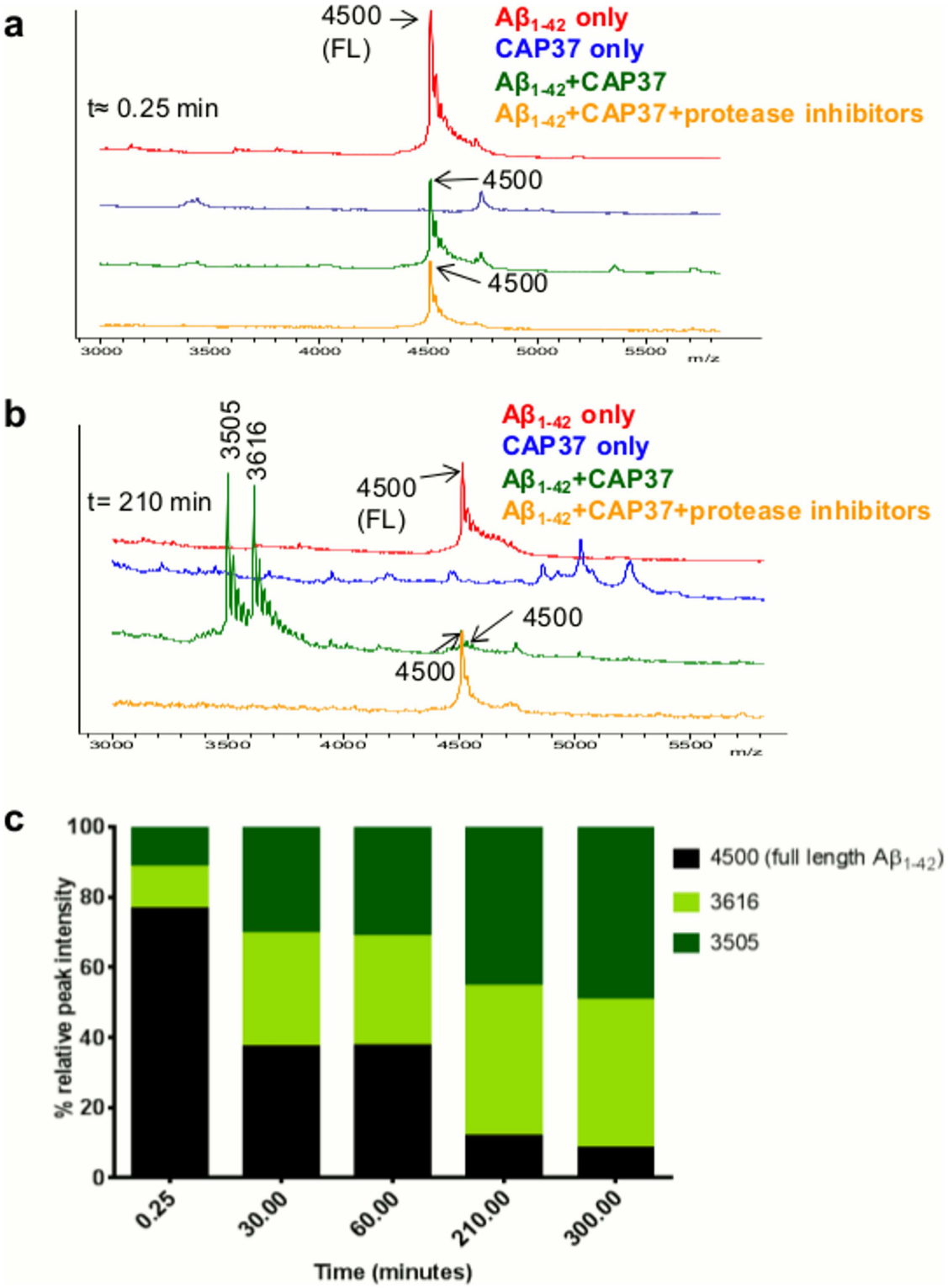

Fig 7. CAP37 slowly cleaves $A\beta_{1-42}$. (a) MALDI-TOF spectra of $A\beta_{1-42}$ that incubated alone (red), with CAP37 (green), or with CAP37+protease inhibitors (orange) at t≈0.25 min. Peaks are labeled with mass-to-charge ratios (m/z), and mass is in Daltons (Da). A peak of 4500 Da, which represents full length (FL) $A\beta_{1-42}$, appears in all $A\beta_{1-42}$ spectra. CAP37 incubated alone is shown in blue, and no peak at 4500 Da is exhibited by CAP37. (b) MALDI-TOF spectra at t = 210 min. Note the reduced size of the full $A\beta_{1-42}$ peak and the presence of two large $A\beta_{1-42}$ fragment peaks at 3616 Da and 3505

Da when $A\beta_{1-42}$ incubated with CAP37. (c) Graph shows % relative peak intensity of $A\beta_{1-42}$ and its fragments (intact $A\beta_{1-42}$ + $A\beta_{1-42}$ fragments) analyzed at t≈ 0.25 min, t = 30 min, t = 60 min, t = 210 min, and t = 300 min. Data are representative of 2 independent experiments.

doi:10.1371/journal.pone.0163330.g007

putative sequences for 2069 Da and 1355 Da. The products at 2069 Da could be either $A\beta_{5-21}$ or $A\beta_{21-42}$ and product 7 could be either $A\beta_{11-21}$ or $A\beta_{12-22}$. Based on sequences confirmed with MS/MS, we demonstrated that neutrophil elastase also cleaved $A\beta_{1-42}$ at Val^{12}-His^{13} and Val^{24}-Gly^{25} (Fig 10b). The fragments generated by cathepsin G were different from those generated by CAP37 and neutrophil elastase. Products at 2072 Da and 2001 Da were not identified with MS/MS, but putative sequences were predicted for each. The product at 2072 Da could be either $A\beta_{5-21}$ or $A\beta_{21-42}$ and product 2 could be either $A\beta_{21-41}$ or $A\beta_{22-42}$. With MS/MS, we identified products 3 and 4 as $A\beta_{15-31}$ and $A\beta_{12-26}$ (Table 4), respectively. Therefore, cathepsin G cleaved $A\beta_{1-42}$ at Glu^{11}-Val^{12}, His^{14}-Gln^{15}, Gly^{25}-Ser^{26}, and Ile^{31}-Ile^{32} (Fig 10c).

Discussion

The current study reveals a novel activity for neutrophil granule proteins CAP37, neutrophil elastase, and cathepsin G. Our data, describe for the first time that these three proteins are capable of disrupting the $A\beta_{1-42}$ -RAGE interaction *in vitro*. Each of the three neutrophil proteins demonstrated distinct affinity and specificity for interacting with either RAGE or $A\beta_{1-42}$. To our surprise, each of the neutrophil proteins also cleaved $A\beta_{1-42}$. The neutrophil proteins disrupted the $A\beta_{1-42}$ -RAGE interaction by competing with $A\beta_{1-42}$ for the same binding site on RAGE, by sequestering $A\beta_{1-42}$ away from RAGE, and/or by degrading $A\beta_{1-42}$. Disruption of the $A\beta_{1-42}$ -RAGE interaction by CAP37 appeared to be primarily due to its sequestering of $A\beta_{1-42}$. Although we show that there is competitive inhibition by CAP37 for $A\beta_{1-42}$ binding RAGE, the high ratio of CAP37: $A\beta_{1-42}$ required for this inhibition makes it un-likely to occur *in vivo*. Since CAP37 cleaved $A\beta_{1-42}$ at a very slow rate, it is also unlikely that CAP37 would disrupt the $A\beta_{1-42}$ –RAGE by cleaving $A\beta_{1-42}$. Disruption by neutrophil elastase was primarily due to proteolytic degradation of $A\beta_{1-42}$ and was not a result of displacement of $A\beta_{1-42}$ from RAGE since no competitive inhibition occurred in the presence of protease inhibitors. It is also unlikely that neutrophil elastase would sequester $A\beta_{1-42}$ since the affinity of $A\beta_{1-42}$ for neutrophil elastase is low. Cathepsin G bound to both RAGE and $A\beta_{1-42}$, and also rapidly degraded $A\beta_{1-42}$. The fact that cathepsin G bound to RAGE, but binding was not significantly reduced with the RAGE antagonist, GM-0111, suggests that this interaction may be due to high electrostatic potential and/or that cathepsin G binds to a non-canonical site on RAGE that is not blocked by the GM-0111 antagonist.

We presume that neutrophil elastase and cathepsin G degraded $A\beta_{1-42}$ due to their serine protease activities. Neutrophil elastase and cathepsin G are classified as serine proteases since they depend on a serine residue for their catalytic activity [31]. Serine proteases have been further classified based on their evolutionary origins. Neutrophil elastase and cathepsin G belong to the PA clan, based on their 3D structure (double β barrel fold) and catalytic triad formed by Histidine (His), Asparagine (Asp), and Serine (Ser) residues [31, 32]. Substrates cleaved by neutrophil elastase and cathepsin G include proteins involved in maintaining the integrity of the extracellular matrix such as fibronectin, laminin, and proteoglycans [33–35]. Neutrophil elastase also cleaves elastin and collagens [35]. Cathepsin G cleaves various proteins involved in blood clotting [36]. In addition, both neutrophil elastase and cathepsin G cleave important immune regulators including complement component 3 [37], complement component 5a receptor (C5aR) [38], and stromal cell-derived factor-1 alpha (SDF-1α) [39, 40]. All six insulin-like growth factor binding proteins, which mediate insulin-like growth factor signaling, are

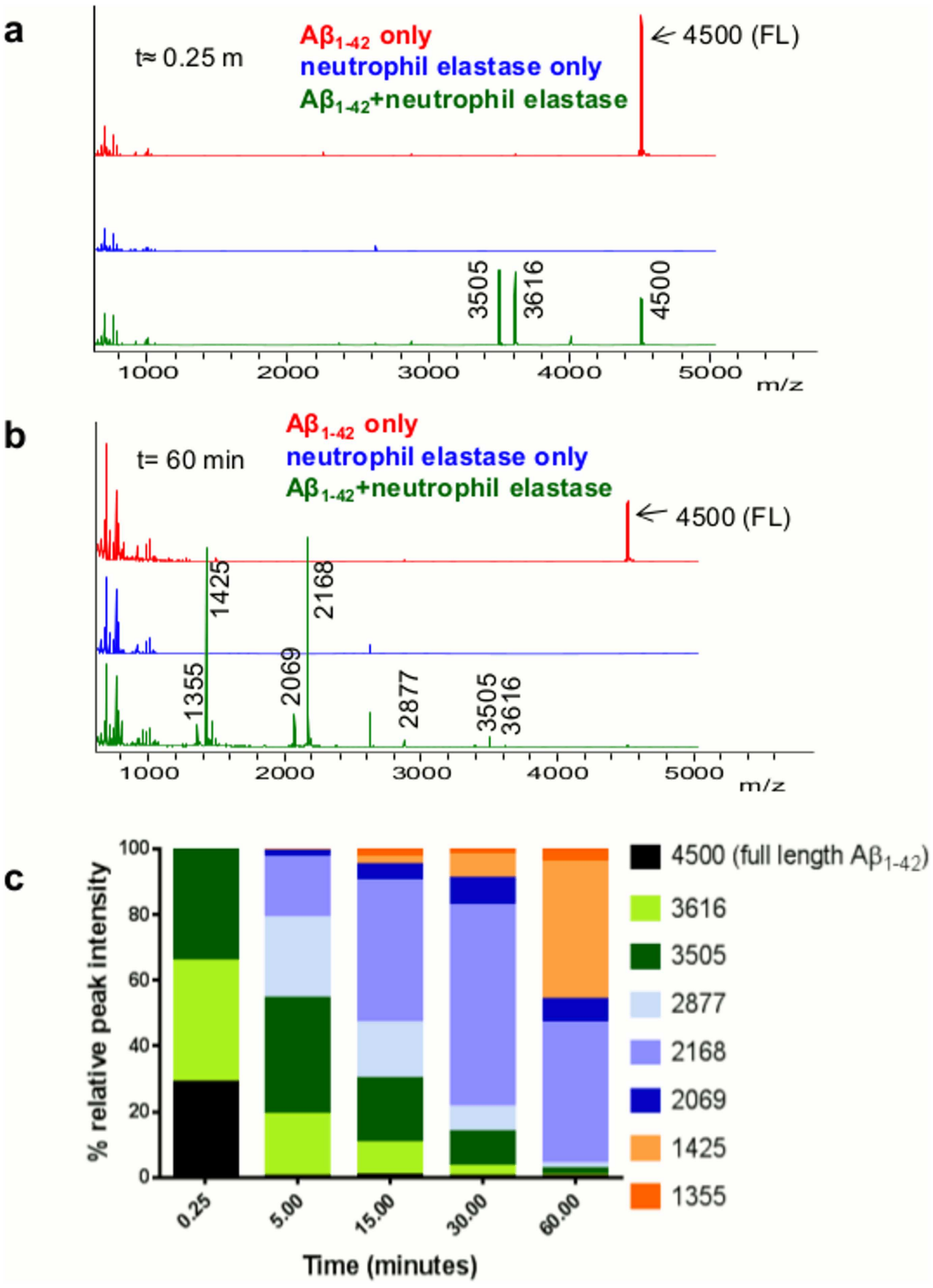

Fig 8. Neutrophil elastase rapidly cleaves $A\beta_{1-42}$. (a) MALDI-TOF spectra of $A\beta_{1-42}$ incubated alone (red) or with neutrophil elastase (green) at t≈0.25 min. Peaks are labeled with mass-to-charge ratios (m/z), and mass is in Daltons (Da). A peak of 4500 Da, which represents intact $A\beta_{1-42}$, appears in all $A\beta_{1-42}$ spectra. Two fragment peaks at 3616 Da and 3505 Da are already present after incubation with neutrophil elastase at t≈0.25 min. Neutrophil elastase incubated alone is shown in blue, and no peak at 4500 Da is exhibited by neutrophil elastase. (b) MALDI-TOF spectra at t = 60 min. Note the reduced size of the full $A\beta_{1-42}$ peak and the peaks at 3616 Da and 3605 Da and the presence of 5 additional fragment peaks at 2877 Da, 2168 Da, 2069 Da, 1425 Da, and 1355 Da when $A\beta_{1-42}$ incubated with neutrophil elastase (green spectra). (c) Graph shows % relative peak intensity of $A\beta_{1-}$

$_{42}$ and its fragments (intact $A\beta_{1-42}$ + $A\beta_{1-42}$ fragments) analyzed at t≈ 0.25 min, t = 5 min, t = 15 min, t = 30 min, and t = 60 min. Data are representative of 3 independent experiments.

doi:10.1371/journal.pone.0163330.g008

also cleaved by neutrophil elastase and cathepsin G [41]. An important consideration is that even though an increase in neutrophil elastase or cathepsin G was not observed in the brains of AD patients in our previous report [10], their enzymatic activities were not determined and may be different in AD patients. Although CAP37 has the same 3D structure as neutrophil elastase and cathepsin G, it has been thought to be an inactive serine protease due to the absence of the conserved His-Asp-Ser catalytic triad replaced by Ser-Asp-Gly [42, 43]. However, recent studies have shown that CAP37 cleaves insulin-like growth factor binding proteins-1,-2, and -4 [44, 45]. Since we demonstrated that CAP37 cleaves Aβ within the C-terminal region, the current study upholds these previous findings indicating that CAP37 does have proteolytic activity. Whether there could be an increase or decrease in CAP37 activity in patients with AD will also need to be determined.

Although other serine proteases including plasmin, myelin basic protein, and acylpeptide hydrolase have been revealed as amyloid beta degrading proteases (AβDPs) [46], this is the first report of neutrophil serine proteases degrading $A\beta_{1-42}$. A previous study demonstrated the ability of cathepsin G to cleave amyloid precursor protein (APP) before the N-terminus of the $A\beta_{1-42}$ peptide [47]. However, degradation of the $A\beta_{1-42}$ peptide itself was not explored. The exact cleavage sites and the kinetics of cleavage were also not investigated in this report. One of the most well-known AβDPs, neprilysin, was found to be identical to skin fibroblast elastase. While both neprilysin and neutrophil elastase have been shown to hydrolyze the premature elastic fibers, oxytalan and elaunin [48], the two enzymes are otherwise distinguishable. Unlike neutrophil elastase, neprilysin is a metalloprotease, and cleaves various peptide hormones including substance P and Bradykinin [49, 50].

The exact sequence of each $A\beta_{1-42}$ fragment formed by cleavage catalyzed by each of the neutrophil proteins is still uncertain, but it is clear that large fragment products are formed first, followed by intermediate sized products, and the smallest products are produced last. Each of the three neutrophil proteins demonstrated distinct kinetics for degrading $A\beta_{1-42}$, and cleaved at different sites within the peptide. All three proteins did cleave at Ile^{31}-Ile^{32}, which was likely one of the initial cleavage sites since the corresponding $A\beta_{1-31}$ is one of the largest products and was formed immediately after $A\beta_{1-42}$ incubation with neutrophil elastase. Cleavage at Val and Gly residues by neutrophil elastase and at Glu, Gln, and His residues by cathepsin G are typical sites of cleavage for these two enzymes [31, 51]. Although we observed $A\beta_{1-31}$ and $A\beta_{1-32}$ products after incubation with CAP37 or neutrophil elastase, we did not observe these products after incubation with cathepsin G. However, it seems possible that these products and others may have been immediately formed and further degraded to form $A\beta_{15-31}$ and $A\beta_{12-26}$ upon incubation with cathepsin G. Since $A\beta_{12-26}$ could not be a cleaved product derived from $A\beta_{15-31}$ or vice versa, it is probable that the two fragments derived from two or more other fragments and were degraded before our analysis. It is uncertain why cathepsin G was truncated to produce a fragment of ~2464 Da only in the presence of $A\beta_{1-42}$ and not when incubated alone. The strong binding of $A\beta_{1-42}$ to cathepsin G could have promoted allosteric regulation of cathepsin G by $A\beta_{1-42}$ causing cathepsin G to be more vulnerable to self-cleavage. It is interesting that CAP37 only cleaved $A\beta_{1-42}$ at Ile residues, because cleavage of insulin-like growth factor binding protein-1 by CAP37 was also found to occur at an Ile residue [44]. The substrate specificity of CAP37 is currently unknown, but based on these findings, it may be possible that CAP37 has a specificity towards hydrophobic aliphatic amino acids. Whether or

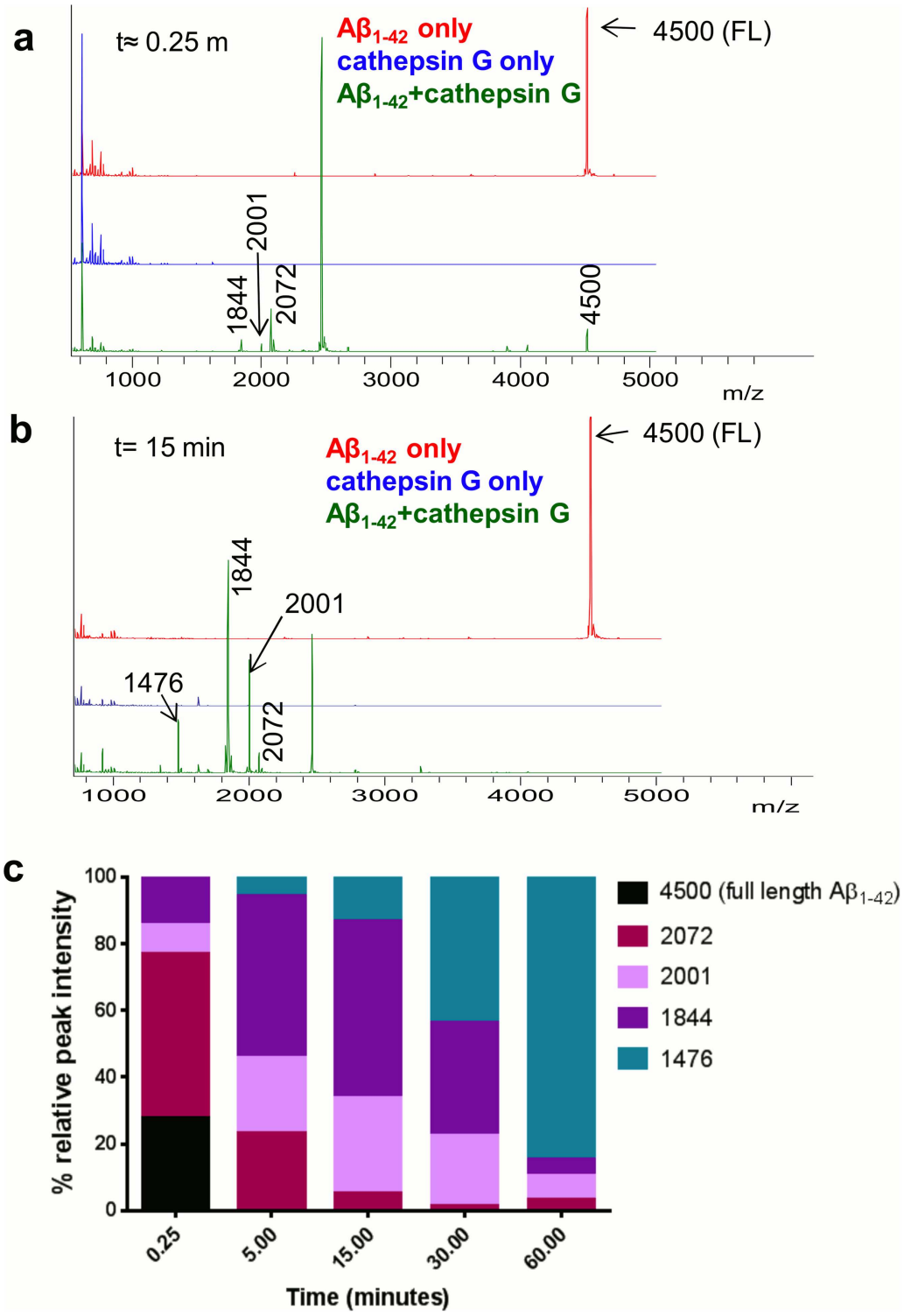

Fig 9. Cathepsin G rapidly cleaves $A\beta_{1-42}$. (a) MALDI-TOF spectra of $A\beta_{1-42}$ incubated alone (red) or with cathepsin G (green) at t≈0.25 min. Peaks are labeled with mass-to-charge ratios (m/z), and mass is in Daltons (Da). A peak of 4500 Da, which represents intact $A\beta_{1-42}$, appears in all $A\beta_{1-42}$ spectra. Peaks predicted to represent $A\beta_{1-42}$ fragments at 2072 Da, 2001 Da, and 1844 Da are already present after incubation with cathepsin G at t≈0.25 min (green). Cathepsin G incubated alone is shown in blue, and no peak at 4500 Da is exhibited by cathepsin G. (b) MALDI-TOF spectra at t = 15 min. Note the absence of the full $A\beta_{1-42}$ peak and the presence of products at 2072 Da, 2001 Da, and 1844 Da as well as an additional fragment peak at 1476 Da

when $A\beta_{1-42}$ incubated with cathepsin G (green). (c) Graph shows relative % peak intensity of $A\beta_{1-42}$ and its fragments (intact $A\beta_{1-42}$ + $A\beta_{1-42}$ fragments at each time point) analyzed at t≈ 0.25 min, t = 5 min, t = 15 min, t = 30 min, and t = 60 min. Data are representative of 3 independent experiments.

doi:10.1371/journal.pone.0163330.g009

not the modified catalytic triad of CAP37 allows for the catalytic activity is unknown. Further studies will be needed to determine the exact mechanism of action.

In a study by Chaney et al., [52] molecular modeling was used to predict that RAGE interacted with the N-terminal domain of Aβ. Our analysis indicates that the N-terminus of $A\beta_{1-42}$ is left intact in the presence of CAP37 but is cleaved by both neutrophil elastase and cathepsin G. This could explain why protease inhibitors prevented neutrophil elastase, but not CAP37, from disrupting binding of $A\beta_{1-42}$ to RAGE (Fig 4). Smaller fragments of $A\beta_{1-42}$ have been demonstrated to be less toxic than the full peptide in cultured brain endothelial cells and SH-SY5Y neuroblastoma cells [53]. Even $A\beta_{1-40}$ is less toxic than $A\beta_{1-42}$ and does not form toxic aggregates as readily [54–56]. Therefore, it is possible that each of the neutrophil proteins could modulate the neurotoxicity of $A\beta_{1-42}$ by degrading it and/or by reducing its interaction with RAGE. Further studies using cell culture and animal models should be conducted to determine the functional outcomes of these neutrophil protein activities.

Only recently have reports began to unveil neutrophils as factors involved in the progression of AD. One study revealed increased numbers of neutrophils in patients with AD as well as in two different transgenic mouse models of AD [57]. Interestingly, depletion of neutrophils was

Table 4. Cleaved $A\beta_{1-42}$ products generated by CAP37, neutrophil elastase, and cathepsin G.

Cleaved $A\beta_{1-42}$ products			
Generated by CAP37			
#	*m/z*	*sequences confirmed by MS/MS*	*product*
1	3616	DAEFRHDSGYEVHHQKLVFFAEDVGSNKGAII	$A\beta_{1-32}$
2	3505	DAEFRHDSGYEVHHQKLVFFAEDVGSNKGAI	$A\beta_{1-31}$
Generated by neutrophil elastase			
#	*m/z*	*sequences confirmed by MS/MS*	*product*
1	3616	DAEFRHDSGYEVHHQKLVFFAEDVGSNKGAII	$A\beta_{1-32}$
2	3505	DAEFRHDSGYEVHHQKLVFFAEDVGSNKGAI	$A\beta_{1-31}$
3	2877	DAEFRHDSGYEVHHQKLVFFAEDV(G)	$A\beta_{1-24}$
6	1425	DAEFRHDSGYEV(H)	$A\beta_{1-12}$
		Putative sequences	
4	2168	Unknown	X
5	2069	1. (F)RHDSGYEVHHQKLVFFA(E) or 2. (F)AEDVGSNKGAIIGLMVGGVIA	1. $A\beta_{5-21}$ or 2. $A\beta_{21-42}$
7	1355	(Y)EVHHQKLVFFA(E) or (E)VHHQKLVFFAE(D)	$A\beta_{11-21}$ or $A\beta_{12-22}$
Generated by cathepsin G			
#	*m/z*	*sequences confirmed by MS/MS*	*product*
3	1844	QKLVFFAEDVGSNKGAI	$A\beta_{15-31}$
4	1476	VHHQKLVFFAEDVG	$A\beta_{12-26}$
		Putative sequences	
1	2072	1. (F)RHDSGYEVHHQKLVFFA(E) or 2. (F)AEDVGSNKGAIIGLMVGGVIA	1. $A\beta_{5-21}$ or 2. $A\beta_{21-42}$
2	2001	1. (F)AEDVGSNKGAIIGLMVGGVI(A) or 2. (A)EDVGSNKGAIIGLMVGGVVIA	1. $A\beta_{21-41}$ or 2. $A\beta_{22-42}$

doi:10.1371/journal.pone.0163330.t004

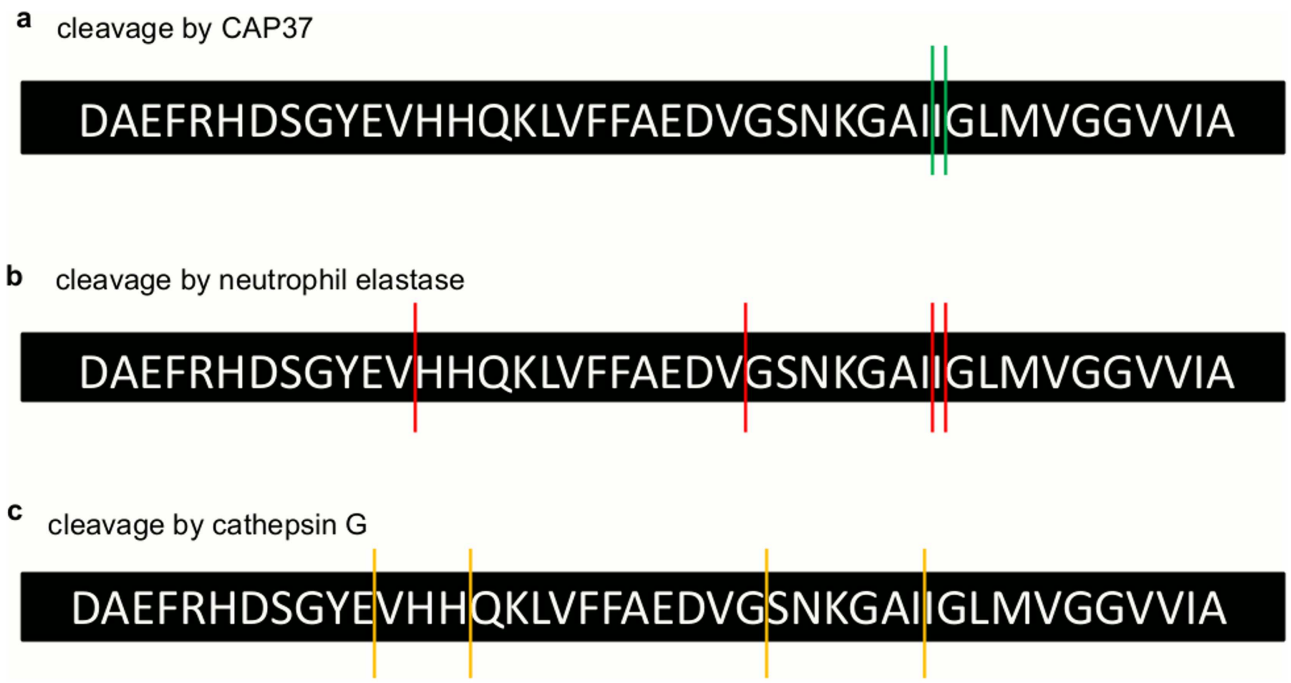

Fig 10. Sites of $A\beta_{1-42}$ cleaved by CAP37, neutrophil elastase, and cathepsin G. Figure shows the sequence of $A\beta_{1-42}$ and the sites at which $A\beta_{1-42}$ is cleaved by (a) CAP37 (green lines), (b) neutrophil elastase (red lines), and (c) cathepsin G (yellow lines).

doi:10.1371/journal.pone.0163330.g010

able to improve memory in transgenic AD mice and reduce pathology, including Aβ load and microgliosis. Another report demonstrated that neutrophils migrated towards Aβ plaques in a mouse model of AD but not in wild-type mice [58]. Our findings that neutrophil proteins are capable of binding and degrading $A\beta_{1-42}$ makes it tempting to speculate whether neutrophils may be migrating toward plaques in an attempt to promote Aβ clearance.

CAP37 may not only be released from neutrophils to interact with Aβ, but may also interact with Aβ inside neurons. Aβ has been reported to accumulate inside neurons and promote dysfunction of organelles [59, 60]. The fact that we previously identified CAP37 expression in neurons signifies a potential interaction between Aβ and CAP37 within neurons. Additional studies are needed to determine if CAP37 could cleave Aβ in neurons or modulate its effects on intracellular organelles. Although neutrophil elastase and cathepsin G have been detected in mouse microglial cells, it is uncertain whether these proteins are expressed within neurons and if they could interact with intraneuronal Aβ.

Possible clearance of Aβ by neutrophils in the periphery could also have important implications. Previous reports have indicated that peripheral clearance of Aβ may reduce Aβ accumulation in the brain [61, 62]. In a recent study by Xiang et al., [63] a mouse model of parabiosis was used in which the bloodstreams of APP transgenic mice were connected to the bloodstreams of wild-type mice. Interestingly, parabiosis significantly reduced blood levels of Aβ as well as brain Aβ plaque burden in the APP transgenic mice compared to APP mice which did not undergo parabiosis. This report indicates that peripheral catabolism of Aβ may be sufficient to prevent its accumulation in the brain. Therapies to effectively promote this catabolism still need to be developed. Neutrophil proteins such as CAP37, neutrophil elastase, and cathepsin G that can sequester or degrade Aβ might support this catabolism.

The current study indicates that CAP37, neutrophil elastase, and cathepsin G may be neuroprotective in the course of AD by decreasing the Aβ-RAGE interaction. However, by binding

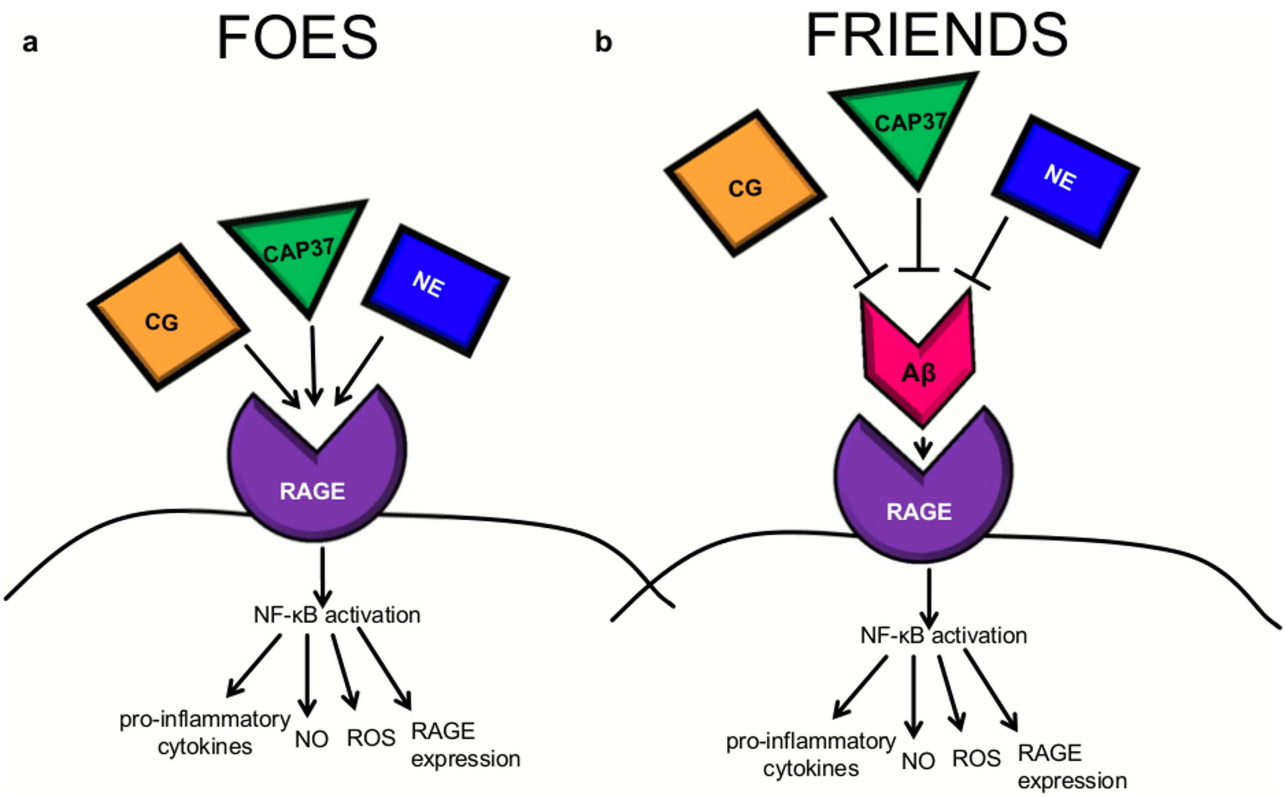

Fig 11. Proposed model for the modulation of RAGE signaling by CAP37, neutrophil elastase, and cathepsin G. (a) CAP37, neutrophil elastase (NE), and/or cathepsin G (CG) may act as RAGE agonists to induce a cell signaling cascade that leads to activation of the transcription factor NF-κB. Activation of NF-κB could then stimulate the production of pro-inflammatory cytokines and pro-oxidants including reactive oxygen species (ROS) and nitric oxide (NO) as well as RAGE itself. In this way, the neutrophil proteins would likely act as foes in the course of chronic inflammatory disease such as AD. (b) CAP37, neutrophil elastase, and cathepsin G may prevent the $A\beta_{1-42}$-RAGE interaction and the corresponding NF-κB signaling cascade. In this way, the neutrophil proteins would act as friends to prevent chronic neuroinflammation driven by $A\beta_{1-42}$ activation of RAGE.

doi:10.1371/journal.pone.0163330.g011

to RAGE, the neutrophil proteins may also be able to act as RAGE agonists to elicit signaling through RAGE independently of their effects on $A\beta_{1-42}$. If this is the case, the neutrophil proteins could act as both friends and foes in the course of chronic neuroinflammatory diseases such as AD (see Fig 11 for hypothetical model).

Conclusions and Future Directions

We conclude that the neutrophil proteins CAP37, neutrophil elastase, and cathepsin G could play an important role in regulating the $A\beta_{1-42}$ -RAGE interaction in cells of the brain and/or periphery. Disrupting this interaction could be neuroprotective in diseases such as AD, in which $A\beta_{1-42}$ -RAGE interactions may contribute to the chronic inflammation, oxidative stress, and brain Aβ accumulation associated with disease pathology. Further studies must be conducted in cell culture and *in vivo* to determine how these proteins could affect neurotoxicity by mediating the $A\beta_{1-42}$ -RAGE interaction. GM-0111 can be utilized in these future studies to determine if the observed effects of neutrophil proteins in cell culture/*in vivo* are RAGE-dependent. Since the GM-0111 not only acts as a RAGE antagonist, but also inhibits the activity of neutrophil elastase, it could also be incorporated into future studies aimed to determine if neutrophil elastase prevents neurotoxicity through its enzymatic activity against $A\beta_{1-42}$.

Acknowledgments

We would like to thank Dr. Arthur Owora, previously a Research Biostatistician of the Department of Pharmaceutical Sciences, University of Oklahoma Health Sciences Center, for his assistance on the statistical analysis performed in this study. We thank Dr. Sixia Chen of the Department of Biostatistics and Epidemiogy, University of Oklahoma Health Sciences Center, for his additional input on the statistical analysis. We thank the Laboratory for Molecular Biology and Cytometry Research at the University of Oklahoma Health Sciences Center for the use of the Core Facility which allowed us to perform the MALDI-TOF MS and MS/MS experiments. GM-0111 was provided as a gift by Dr. Justin Savage, GlycoMira Therapeutics, Inc.

Author Contributions

Conceptualization: HAP AKJ AJS.

Data curation: AJS JDW.

Formal analysis: AJS.

Funding acquisition: HAP AKJ.

Investigation: AJS AKJ JDW VHS.

Methodology: AJS AKJ JDW VHS GDP HAP.

Project administration: HAP.

Resources: GDP HAP.

Software: JDW.

Supervision: HAP.

Validation: AJS AKJ HAP VHS.

Visualization: AJS AKJ HAP JDW.

Writing – original draft: AJS AKJ.

Writing – review & editing: AJS AKJ JDW VHS GDP HAP.

References

1. Pham CT. Neutrophil serine proteases: specific regulators of inflammation. Nat Rev. Immunol 2006; 6 (7):541–550. PMID: 16799473
2. Pereira HA, Ruan X, Kumar P. Activation of microglia: a neuroinflammatory role for CAP37. Glia. 2003; 41(1):64–72. PMID: 12465046
3. Meyer-Hoffert U, Wiedow O. Neutrophil serine proteases: mediators of innate immune responses. Curr Opin Hematol. 2011; 18(1):19–24. PMID: 21042214
4. Korkmaz B, Horwitz MS, Jenne DE, Gauthier F. Neutrophil elastase, proteinase 3, and cathepsin G as therapeutic targets in human diseases. Pharmacological reviews. 2010; 62(4):726–759. doi: 10.1124/pr.110.002733 PMID: 21079042
5. Harris MG, Hulseberg P, Ling C, Karman J, Clarkson BD, Harding JS, et al. Immune privilege of the CNS is not the consequence of limited antigen sampling. Sci Rep. 2014; 4:4422. doi: 10.1038/srep04422 PMID: 24651727
6. Louveau A, Harris TH, Kipnis J. Revisiting the Mechanisms of CNS Immune Privilege. Trends Immunol. 2015; 36(10):569–577. doi: 10.1016/j.it.2015.08.006 PMID: 26431936
7. Lefkowitz DL, Lefkowitz SS. Microglia and myeloperoxidase: a deadly partnership in neurodegenerative disease. Free Radic Biol Med. 2008; 45(5):726–731. doi: 10.1016/j.freeradbiomed.2008.05.021 PMID: 18554520

8. Watt AD, Perez KA, Ang CS, O'Donnell P, Rembach A, Pertile KK, et al. Peripheral alpha- defensins 1 and 2 are elevated in Alzheimer's disease. Journal of Alzheimer's disease: JAD. 2015; 44(4):1131–1143. doi: 10.3233/JAD-142286 PMID: 25408207
9. Pereira HA, Kumar P, Grammas P. Expression of CAP37, a novel inflammatory mediator, in Alzheimer's disease. Neurobiology of aging. 1996; 17(5):753–759. PMID: 8892348
10. Brock AJ, Kasus-Jacobi A, Lerner M, Logan S, Adesina AM, Anne Pereira H. The antimicrobial protein, CAP37, is upregulated in pyramidal neurons during Alzheimer's disease. Histochem Cell Biol. 2015; 144(4):293–308. doi: 10.1007/s00418-015-1347-x PMID: 26170148
11. Wren JD. A global meta-analysis of microarray expression data to predict unknown gene functions and estimate the literature-data divide. Bioinformatics. 2009; 25(13):1694–1701. doi: 10.1093/bioinformatics/btp290 PMID: 19447786
12. Kierdorf K, Fritz G. RAGE regulation and signaling in inflammation and beyond. Journal of leukocyte biology. 2013; 94(1):55–68. doi: 10.1189/jlb.1012519 PMID: 23543766
13. Bierhaus A, Humpert PM, Morcos M, Wendt T, Chavakis T, Arnold B, et al. Understanding RAGE, the receptor for advanced glycation end products. J Mol Med (Berl). 2005; 83(11):876–886.
14. Fritz G. RAGE: a single receptor fits multiple ligands. Trends Biochem Sci. 2011; 36(12):625–632. doi: 10.1016/j.tibs.2011.08.008 PMID: 22019011
15. Gonzalez-Reyes RE, Graciela Rubiano M. Astrocyte's RAGE: More Than Just a Question of Mood. Cent Nerv Syst Agents Med Chem. 2016.
16. Xie J, Mendez JD, Mendez-Valenzuela V, Aguilar-Hernandez MM. Cellular signalling of the receptor for advanced glycation end products (RAGE). Cell Signal. 2013; 25(11):2185–2197. doi: 10.1016/j.cellsig.2013.06.013 PMID: 23838007
17. Yan SD, Chen X, Fu J, Chen M, Zhu H, Roher A, et al.RAGE and amyloid-beta peptide neurotoxicity in Alzheimer's disease. Nature. 1996; 382(6593):685–691. PMID: 8751438
18. Cummings JL. Alzheimer's disease. N Engl J Med. 2004; 351(1):56–67. PMID: 15229308
19. Murphy MP, LeVine H 3rd. Alzheimer's disease and the amyloid-beta peptide. Journal of Alzheimer's disease: JAD. 2010; 19(1):311–323. doi: 10.3233/JAD-2010-1221 PMID: 20061647
20. Carrano A, Hoozemans JJ, van der Vies SM, Rozemuller AJ, van Horssen J, de Vries HE. Amyloid Beta induces oxidative stress-mediated blood-brain barrier changes in capillary amyloid angiopathy. Antioxid Redox. Signal 2011; 15(5):1167–1178. doi: 10.1089/ars.2011.3895 PMID: 21294650
21. Askarova S, Yang X, Sheng W, Sun GY, Lee JC. Role of Abeta-receptor for advanced glycation end-products interaction in oxidative stress and cytosolic phospholipase A(2) activation in astrocytes and cerebral endothelial cells. Neuroscience. 2011; 199:375–385. PMID: 21978883
22. Deane R, Singh I, Sagare AP, Bell RD, Ross NT, LaRue B, et al. A multimodal RAGE- specific inhibitor reduces amyloid beta-mediated brain disorder in a mouse model of Alzheimer disease. The Journal of clinical investigation. 2012; 122(4):1377–1392. doi: 10.1172/JCI58642 PMID: 22406537
23. Du Yan S, Zhu H, Fu J, Yan SF, Roher A, et al. Amyloid-beta peptide-receptor for advanced glycation endproduct interaction elicits neuronal expression of macrophage-colony stimulating factor: a proinflammatory pathway in Alzheimer disease. Proceedings of the National Academy of Sciences of the United States of America. 1997; 94(10):5296–5301. PMID: 9144231
24. Lee WY, Savage JR, Zhang J, Jia W, Oottamasathien S, Prestwich GD. Prevention of anti- microbial peptide LL-37-induced apoptosis and ATP release in the urinary bladder by a modified glycosaminoglycan. PloS one. 2013; 8(10):e77854. doi: 10.1371/journal.pone.0077854 PMID: 24204996
25. Barrett T, Troup DB, Wilhite SE, Ledoux P, Rudnev D, Evangelista C, et al. NCBI GEO: mining tens of millions of expression profiles—database and tools update. Nucleic Acids Res. 2007; 35(Database issue):D760–765. PMID: 17099226
26. Goel R, Harsha HC, Pandey A, Prasad TSK. Human Protein Reference Database and Human Proteinpedia as resources for phosphoproteome analysis. Mol Biosyst. 2012; 8(2):453–463. doi: 10.1039/c1mb05340j PMID: 22159132
27. Donato R, Cannon BR, Sorci G, Riuzzi F, Hsu K, Weber DJ, et al. Functions of S100 proteins. Curr Mol Med. 2013; 13(1):24–57. PMID: 22834835
28. Ryckman C, Vandal K, Rouleau P, Talbot M, Tessier PA. Proinflammatory activities of S100: proteins S100A8, S100A9, and S100A8/A9 induce neutrophil chemotaxis and adhesion. J Immunol. 2003; 170(6):3233–3242. PMID: 12626582
29. Abtin A, Eckhart L, Glaser R, Gmeiner R, Mildner M, Tschachler E. The antimicrobial heterodimer S100A8/S100A9 (calprotectin) is upregulated by bacterial flagellin in human epidermal keratinocytes. J Invest Dermatol. 2010; 130(10):2423–2430. doi: 10.1038/jid.2010.158 PMID: 20555353

30. Narumi K, Miyakawa R, Ueda R, Hashimoto H, Yamamoto Y, Yoshida T, et al. Proinflammatory Proteins S100A8/S100A9 Activate NK Cells via Interaction with RAGE. J Immunol. 2015; 194(11):5539–5548. doi: 10.4049/jimmunol.1402301 PMID: 25911757

31. Di Cera E. Serine proteases. IUBMB Life. 2009; 61(5):510–515. doi: 10.1002/iub.186 PMID: 19180666

32. Barrett AJ, Rawlings ND. Families and clans of serine peptidases. Arch Biochem Biophys. 1995; 318 (2):247–250. PMID: 7733651

33. Masood A, Yi M, Belcastro R, Li J, Lopez L, Kantores C, Jankov RP, Tanswell AK. Neutrophil elastase-induced elastin degradation mediates macrophage influx and lung injury in 60% O2-exposed neonatal rats. Am J Physiol Lung Cell Mol Physiol. 2015; 309(1):L53–62. doi: 10.1152/ajplung.00298.2014 PMID: 26136527

34. McDonald JA, Kelley DG. Degradation of fibronectin by human leukocyte elastase. Release of biologically active fragments. The Journal of biological chemistry. 1980; 255(18):8848–8858. PMID: 6902725

35. Owen CA, Campbell EJ. The cell biology of leukocyte-mediated proteolysis. Journal of leukocyte biology. 1999; 65(2):137–150. PMID: 10088596

36. Turkington PT. Cathepsin G, a regulator of human vitamin K, dependent clotting factors and inhibitors. Thromb Res. 1992; 67(2):147–155. PMID: 1440518

37. Maison CM, Villiers CL, Colomb MG. Proteolysis of C3 on U937 cell plasma membranes. Purification of cathepsin G. J Immunol. 1991; 147(3):921–926. PMID: 1861080

38. van den Berg CW, Tambourgi DV, Clark HW, Hoong SJ, Spiller OB, McGreal EP. Mechanism of neutrophil dysfunction: neutrophil serine proteases cleave and inactivate the C5a receptor. J Immunol. 2014; 192(4):1787–1795. doi: 10.4049/jimmunol.1301920 PMID: 24446515

39. Valenzuela-Fernandez A, Planchenault T, Baleux F, Staropoli I, Le-Barillec K, Leduc D, et al. Leukocyte elastase negatively regulates Stromal cell-derived factor-1 (SDF-1)/CXCR4 binding and functions by amino-terminal processing of SDF-1 and CXCR4. The Journal of biological chemistry. 2002; 277 (18):15677–15689. PMID: 11867624

40. Delgado MB, Clark-Lewis I, Loetscher P, Langen H, Thelen M, Baggiolini M, et al. Rapid inactivation of stromal cell-derived factor-1 by cathepsin G associated with lymphocytes. Eur J Immunol. 2001; 31 (3):699–707. PMID: 11241273

41. Gibson TL, Cohen P. Inflammation-related neutrophil proteases, cathepsin G and elastase, function as insulin-like growth factor binding protein proteases. Growth Horm IGF Res. 1999; 9(4):241–253. PMID: 10512690

42. Olczak M, Indyk K, Olczak T. Reconstitution of human azurocidin catalytic triad and proteolytic activity by site-directed mutagenesis. Biol Chem. 2008; 389(7):955–962. doi: 10.1515/BC.2008.101 PMID: 18627314

43. Morgan JG, Pereira HA, Sukiennicki T, Spitznagel JK, Larrick JW. Human neutrophil granule cationic protein CAP37 is a specific macrophage chemotaxin that shares homology with inflammatory proteinases. Adv Exp Med Biol. 1991; 305:89–96. PMID: 1755383

44. Wang J, Shafqat J, Hall K, Stahlberg M, Wivall-Helleryd IL, Bouzakri K, Zierath JR, et al. Specific cleavage of insulin-like growth factor-binding protein-1 by a novel protease activity. Cell Mol Life Sci. 2006; 63(19–20):2405–2414. PMID: 17006628

45. Brandt K, Lundell K, Brismar K. Neutrophil-derived azurocidin cleaves insulin-like growth factor-binding protein-1, -2 and -4. Growth Horm IGF Res. 2011; 21(3):167–173. doi: 10.1016/j.ghir.2011.04.003 PMID: 21550830

46. Saido T, Leissring MA. Proteolytic degradation of amyloid beta-protein. Cold Spring Harbor perspectives in medicine. 2012; 2(6):a006379. doi: 10.1101/cshperspect.a006379 PMID: 22675659

47. Savage MJ, Iqbal M, Loh T, Trusko SP, Scott R, Siman R. Cathepsin G: localization in human cerebral cortex and generation of amyloidogenic fragments from the beta-amyloid precursor protein. Neuroscience. 1994; 60(3):607–619. PMID: 7936190

48. Godeau G, Hornebeck W. Morphometric analysis of the degradation of human skin elastic fibres by human leukocyte elastase (EC 3-4-21-37) and human skin fibroblast elastase (EC 3–4–24). Pathol Biol (Paris). 1988; 36(9):1133–1138.

49. Skidgel RA, Erdos EG. Angiotensin converting enzyme (ACE) and neprilysin hydrolyze neuropeptides: a brief history, the beginning and follow-ups to early studies. Peptides. 2004; 25(3):521–525. PMID: 15134871

50. Erdos EG, Skidgel RA: Neutral endopeptidase 24.11 (enkephalinase) and related regulators of peptide hormones. FASEB journal: official publication of the Federation of American Societies for Experimental Biology. 1989; 3(2):145–151.

51. Aimetti AA, Tibbitt MW, Anseth KS. Human neutrophil elastase responsive delivery from poly(ethylene glycol) hydrogels. Biomacromolecules. 2009; 10(6):1484–1489. doi: 10.1021/bm9000926 PMID: 19408953

52. Chaney MO, Stine WB, Kokjohn TA, Kuo YM, Esh C, Rahman A, et al. RAGE and amyloid beta interactions: atomic force microscopy and molecular modeling. Biochim Biophys Acta. 2005; 1741(1–2):199–205. PMID: 15882940

53. Hernandez-Guillamon M, Mawhirt S, Blais S, Montaner J, Neubert TA, Rostagno A, et al. Sequential Amyloid-beta Degradation by the Matrix Metalloproteases MMP-2 and MMP-9. The Journal of biological chemistry. 2015; 290(24):15078–15091. doi: 10.1074/jbc.M114.610931 PMID: 25897080

54. Pauwels K, Williams TL, Morris KL, Jonckheere W, Vandersteen A, Kelly G, et al. Structural basis for increased toxicity of pathological abeta42:abeta40 ratios in Alzheimer disease. The Journal of biological chemistry. 2012; 287(8):5650–5660. doi: 10.1074/jbc.M111.264473 PMID: 22157754

55. Kuperstein I, Broersen K, Benilova I, Rozenski J, Jonckheere W, Debulpaep M, et al. Neurotoxicity of Alzheimer's disease Abeta peptides is induced by small changes in the Abeta42 to Abeta40 ratio. EMBO J. 2010; 29(19):3408–3420. doi: 10.1038/emboj.2010.211 PMID: 20818335

56. Chen YR, Glabe CG. Distinct early folding and aggregation properties of Alzheimer amyloid-beta peptides Abeta40 and Abeta42: stable trimer or tetramer formation by Abeta42. The Journal of biological chemistry. 2006; 281(34):24414–24422. PMID: 16809342

57. Zenaro E, Pietronigro E, Della Bianca V, Piacentino G, Marongiu L, Budui S, et al. Neutrophils promote Alzheimer's disease-like pathology and cognitive decline via LFA-1 integrin. Nature medicine. 2015; 21(8):880–886. doi: 10.1038/nm.3913 PMID: 26214837

58. Baik SH, Cha MY, Hyun YM, Cho H, Hamza B, Kim DK, et al. Migration of neutrophils targeting amyloid plaques in Alzheimer's disease mouse model. Neurobiology of aging. 2014; 35(6):1286–1292. doi: 10.1016/j.neurobiolaging.2014.01.003 PMID: 24485508

59. Ditaranto K, Tekirian TL, Yang AJ. Lysosomal membrane damage in soluble Abeta- mediated cell death in Alzheimer's disease. Neurobiol Dis. 2001; 8(1):19–31. PMID: 11162237

60. Almeida CG, Takahashi RH, Gouras GK. Beta-amyloid accumulation impairs multivesicular body sorting by inhibiting the ubiquitin-proteasome system. J Neurosci. 2006; 26(16):4277–4288. PMID: 16624948

61. Marques MA, Kulstad JJ, Savard CE, Green PS, Lee SP, Craft S,et al. Peripheral amyloid- beta levels regulate amyloid-beta clearance from the central nervous system. Journal of Alzheimer's disease: JAD. 2009; 16(2):325–329. doi: 10.3233/JAD-2009-0964 PMID: 19221422

62. DeMattos RB, Bales KR, Cummins DJ, Dodart JC, Paul SM, Holtzman DM. Peripheral anti- A beta antibody alters CNS and plasma A beta clearance and decreases brain A beta burden in a mouse model of Alzheimer's disease. Proceedings of the National Academy of Sciences of the United States of America. 2001; 98(15):8850–8855. PMID: 11438712

63. Xiang Y, Bu XL, Liu YH, Zhu C, Shen LL, Jiao SS, et al. Physiological amyloid-beta clearance in the periphery and its therapeutic potential for Alzheimer's disease. Acta neuropathologica. 2015; 130 (4):487–499. doi: 10.1007/s00401-015-1477-1 PMID: 26363791